Article

Superior Pyrimidine Derivatives as Selective ABCG2 Inhibitors and Broad-spectrum ABCB1, ABCC1, and ABCG2 Antagonists

Katja Silbermann, Jiyang Li, Vigneshwaran Namasivayam, Fabian Baltes, Gerd Bendas, Sven Marcel Stefan, and Michael Wiese

J. Med. Chem., **Just Accepted Manuscript** • DOI: 10.1021/acs.jmedchem.0c00961 • Publication Date (Web): 31 Jul 2020

Superior Pyrimidine Derivatives as Selective ABCG2 Inhibitors and Broad-spectrum ABCB1, ABCC1, and ABCG2 Antagonists.

Katja Silbermann[#], Jiyang Li[#], Vigneshwaran Namasivayam, Fabian Baltes, Gerd Bendas, Sven Marcel Stefan, Michael Wiese**

Pharmaceutical and Cellbiological Chemistry, Pharmaceutical Institute, Rheinische Friedrich-Wilhelms-University Bonn, An der Immenburg 4, 53121 Bonn, Germany

Key Words. ABC transporter; ABCG2 (BCRP) inhibition; ABCB1 (P-gp); ABCC1 (MRP1); Multidrug Resistance (MDR); triple (multi-target) inhibitor.

# These two authors contributed equally to this work

* Corresponding authors: Michael Wiese (mwiese@uni-bonn.de)

Sven Marcel Stefan (s.m.stefan@medisin.uio.no)

Abstract

In search for highly effective modulators addressing ABCG2-mediated MDR, 23 pyrimidines were synthesized and biologically assessed. Seven derivatives with (a) nitrogen- and/or halogen-containing residue(s) had extraordinary potencies against ABCG2 (IC_{50} < 150 nM). The compounds competitively inhibited ABCG2-mediated Hoechst 33342 transport, but were not substrates of ABCG2. The most potent MDR

reverser compound **19** concentration-dependently increased SN-38-mediated cancer cell death at 11 nM (EC_{50}), time-dependently doubled SN-38 toxicity in a period of seven days at 10 nM, and half-maximally accelerated cell death combined with SN-38 at 17 nM. No induction of ABCG2 was observed. Furthermore, eleven pyrimidines were revealed as triple ABCB1/ABCC1/ABCG2 inhibitors. Five possessed IC_{50} values below 10 μM against each transporter, classifying them as some of the 50 most potent multi-target ABC transporter inhibitors. The most promising representative compound **37** reversed ABCB1-, ABCC1-, and ABCG2-mediated MDR, making it one of the 3 most potent ABC transporter inhibitors and reversers of ABC-transporters-mediated MDR.

Introduction

Multidrug resistance (MDR) in cancer chemotherapy remains until today a major obstacle in oncology.[1] In both chemo-naive[2,3] as well as chemo-treated patients,[4,5] the overexpression of ATP-binding cassette (ABC) transport proteins is associated with a negative prognosis and poor outcome of first-line chemotherapeutic intervention. Recurrence of certain cancers, such as leukemia,[4,6,7] as well as lung,[2] pancreatic,[8] ovarian,[3,9] or breast cancer[10,11] was already connected to the overexpression of ABC transporters.[3,6,7,8,10,11] These efflux pumps are not only negative prognostic markers for the development of metastasis,[12] but collectively lead to decreased progression- and disease-free survival as well as increased mortality.[3,6,7,8,9,10,11] One of the most important representatives in this regard is ABCG2 (breast cancer resistance protein; BCRP).[6,7,8] ABCG2 confers resistance to a broad spectrum of chemically unrelated

anticancer drugs, such as camptothecins, epipodophyllotoxins, mitoxantrone, and tyrosine kinase inhibitors (TKIs).[13,14] Overexpression of this ABC transporter was found in several cancer cell lines derived from leukemia, as well as cancers from lung, ovary, colon, prostate gland, or breast.[13,15] One strategy to treat certain advanced and/or relapsed cancers is the use of camptothecin (**1**; Figure 1) analogs [e.g., topotecan (**2**; Figure 1),[16,17] or irinotecan (**3**; Figure 1)[18]] as second-line treatment. However, cell lines derived from certain malignancies acquired ABCG2 expression[19,20] after exposure to **1**[21] and its analogs **2**[20,22,23] and **3**[24] as well as its active metabolite SN-38 (**4**; Figure 1),[24,25] leading to cross-resistance.[20,21,22,23,24,25] Other tumor cell lines even showed inherent ABCG2 expression and resistance toward camptothecins.[26] One concept to overcome resistance against **1** in certain cancers was the design of compound **1** analogs that were less recognized by ABCG2, which led to promising candidates, such as diflomotecan,[27] gimatecan,[28] or lurtotecan.[29] Nonetheless, ABCG2-overexpressing cells always possessed a basic (cross-)resistance against these agents that could not be abolished by structural variations.[24,29,30,31] In addition, certain representatives were shown to induce ABCG2 on mRNA and protein levels.[30,31]

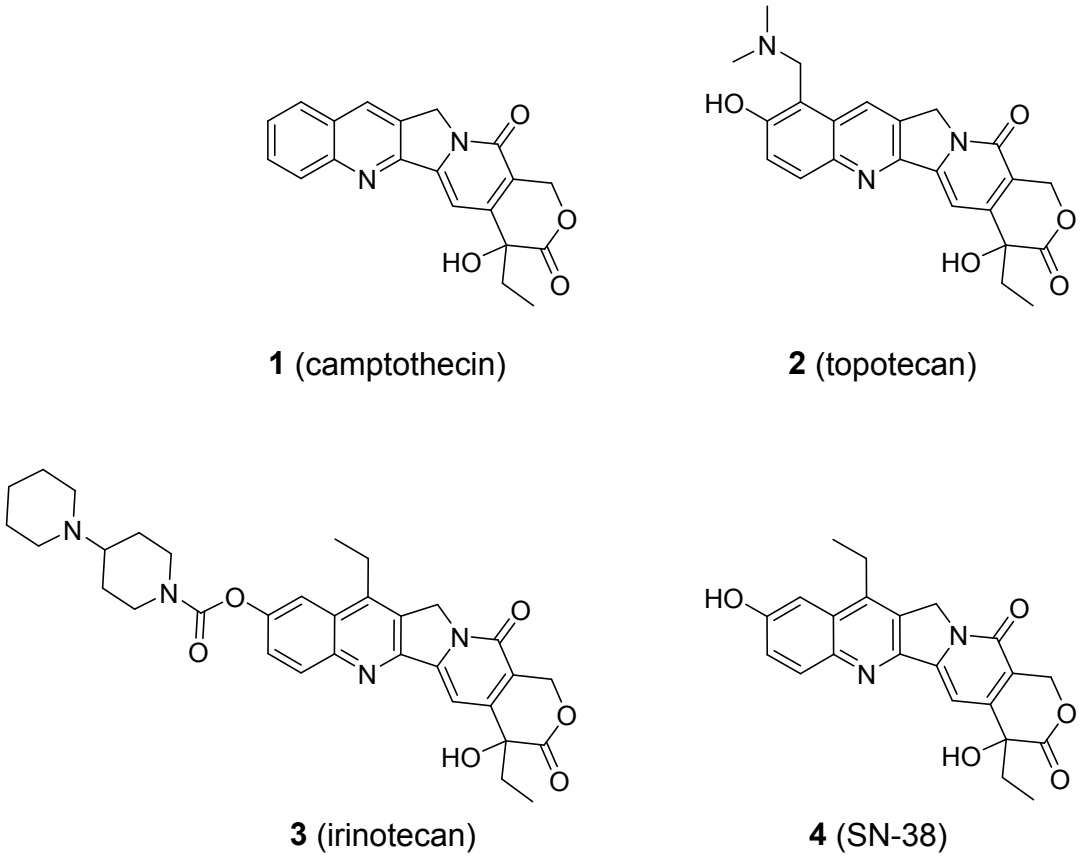

Figure 1: Compound **1** and its derivatives commonly used in second-line anticancer regimens.

Another approach was the design of inhibitors of ABCG2 which blocked the efflux of compound **1** analogs and increased their persistence inside of cancer cells. Several tyrosine kinase inhibitors were proven to reverse ABCG2-mediated resistance against camptothecins.[14] This was firstly described for canertinib (**5**; Figure 2),[32] which reversed ABCG2-mediated resistance against **4**. Until today, only very few TKIs did likewise at low triple-digit to high double-digit nanomolar concentrations,[33,34,35,36,37] such as ceritinib (**6**; Figure 2).[38] Most compounds exerted their reversing potential in the micromolar concentration range, and clinical evaluations of TKIs in combination

with either **2**[39,40,41] or **3**[42,43,44,45,46] had only limited success. This was attributed to no benefit of the combination compared to single-drug treatment[40,43,46] and/or severe adverse side effects.[39,41,42,44,45,46]

In need of the development of more potent and less adverse side effects-associated adjuvant modulators of ABCG2-related cancers, a bulk of compounds were generated on the basis of the main scaffolds of TKIs. These were mostly either quinazoline,[32,33,36,47] quinoline,[35,48,49] pyrimidine[38,50,51] or pyridine[37,52] derivatives. Subsequent optimization of the backbone derived from compound **5**[32] resulted in either highly potent quinazoline-containing (e.g., **7**; Figure 2),[53,54] or broad-spectrum quinoline-containing ABCG2 inhibitors (e.g., **8**; Figure 2).[55] Further improvement resulted in the most potent ABCG2-mediated MDR-reverser known until today (**9**; EC_{50} = 12.7 nM; Figure 2).[56] The most recent and final improvement was the downsizing of the structures to a pyrimidine scaffold, yielding highly potent ABCG2 inhibitors and reversers of ABCG2-mediated MDR (e.g., **10**; Figure 2).[57]

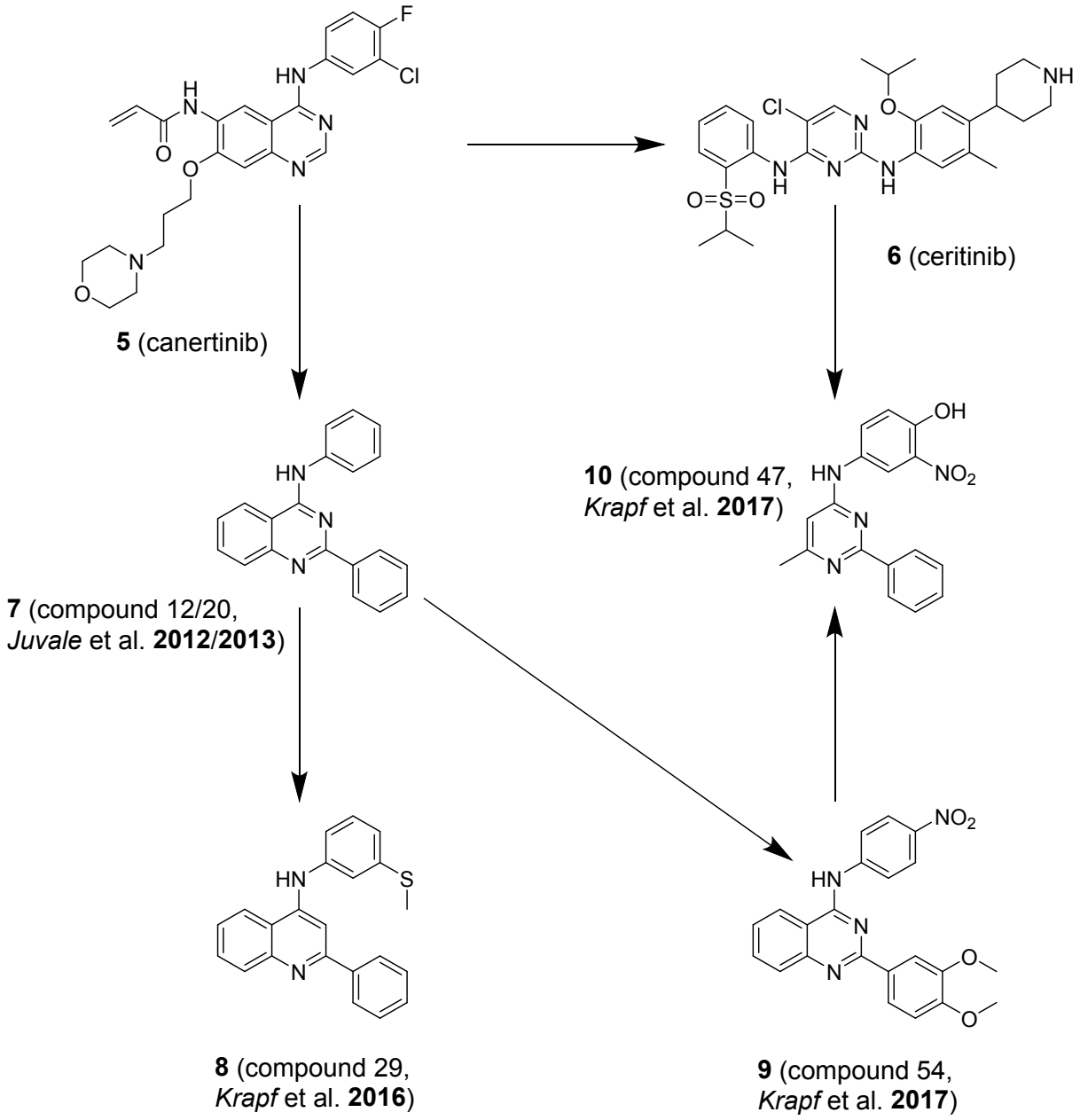

Figure 2: Depiction of inhibitor- and MDR reverser-development regarding ABCG2-mediated drug transport; compound **5**: very first TKI associated with inhibition of ABCG2 and reversal of ABCG2-mediated compound **1** analog resistance;[32] compound **6**: most active TKI regarding MDR reversal against topotecan in ABCG2-overexpressing cells (EC_{50} = ~65 nM);[38] compound **7**: one of the first reported HTS-derived quinazolines as ABCG2 inhibitors;[53,54] compound **8**: exceptional

representative of a triple ABCB1/ABCC1/ABCG2 inhibitor;[55] compound **9**: one of the most potent ABCG2-mediated MDR reversers known until today (EC_{50} = 12.7 nM);[56,57] compound **10**: one of only 7 synthetic pyrimidine derivatives as ABCG2 inhibitors.[57]

As only 7 pyrimidine derivatives have been described as ABCG2 inhibitors in literature,[57] the aim of the present study was further exploration of the pyrimidine class as ABCG2 inhibitors. The substitution pattern has carefully been selected according to our experience from previous studies[53,54,55,56,57,58,59,60,61] as well as reports of TKIs targeting ABCG2.[32,33,36,39,40,47,48,52] This included introduction of flexible nitrogen-(cyano or nitro)- and oxygen-(hydroxy or methoxy)-containing substituents with or without combination of halogens (fluorine, chlorine, bromine), but also bulky, rigid nitrogen- and oxygen containing heterocycles. Compounds with high inhibitory power, low cytotoxicity, highly effective MDR reversal capability, and ABCG2-selectivity were in focus, neither being substrates of this transporter, nor interfering with its expression. As our past investigations frequently led to the discovery of multi-target ABCB1, ABCC1, and ABCG2 inhibitors,[54,55,61,62,63,64,65,66] a second task of the present work was the screening of the 23 synthesized compounds against ABCB1 and ABCC1 as well as evaluating their capability to reverse ABCB1-, ABCC1-, and ABCG2-mediated MDR. As certain cancers simultaneously overexpress specific ABC transporters,[67,68] and selective inhibition and/or downregulation of one transporter (e.g. ABCG2) might lead to compensatory up-regulation of another (e.g., ABCB1 and/or ABCC1),[69,70,71] broad-spectrum ABC transporter inhibitors are considered to be useful tools in a novel

strategy to approach multidrug-resistant cancers.[72,73] However, until today only ~1000 compounds have been evaluated regarding inhibition of ABCB1, ABCC1, and ABCG2. This group of compounds comprised of less than 120 triple ABCB1/ABCC1/ABCG2 inhibitors, less than 50 of these exerting their effect at 10 µM or lower,[38,49,54,55,61,62,63,64,65,66,74,75,76,77,78,79,80,81,82,83,84] and less than 20 compounds at 5 µM or lower against all three transporters.[55,63,74,77,78,79,80,82,83] While ~75 compounds were reported in the literature as reversers of ABCB1-, ABCC1-, and ABCG2-mediated MDR,[47,48,50,50,52,65,66,85,86,87,88,89] only 2 compounds have been proven to exert their MDR reversing effect due to inhibition of these ABC transporters, 9-deazapurine 55 (**11**; Figure 3) and thienopyrimidine 14 (**12**, Figure 3).[65,66]

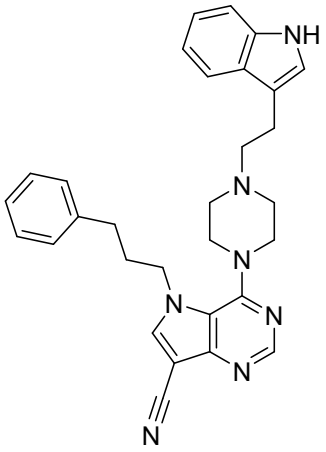

11 (compound 55, *Stefan* et al. **2017**)

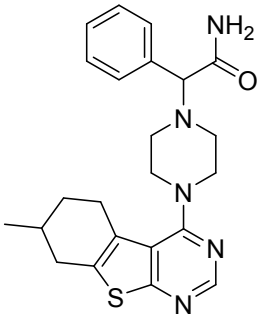

12 (compound 14, *Silbermann* et al. **2019**)

Figure 3: Reported triple reversers of ABCB1-, ABCC1-, and ABCG2-mediated MDR that proved to exert their effect due to inhibition of ABCB1, ABCC1, and ABCG2: 9-deazapurine 55 (**11**)[65] and thienopyrimidine 14 (**12**).[66]

Results and Discussion

Chemistry

Synthesis of 4-anilino-6-methyl-2-phenylpyrimidine derivatives was achieved in three steps as depicted in Scheme 1. First, a Pinner pyrimidine synthesis was applied by condensing a benzamidine with ethyl acetoacetate in a freshly prepared sodium ethoxide solution to form the pyrimidine ring (**13**). Exposure to excess phosphoryl chloride yielded 4-chloro-6-methyl-2-phenylpyrimidine (**14**). Finally, the chlorinated pyrimidine was reacted with differently substituted anilines to obtain the desired products (**18**-**40**).

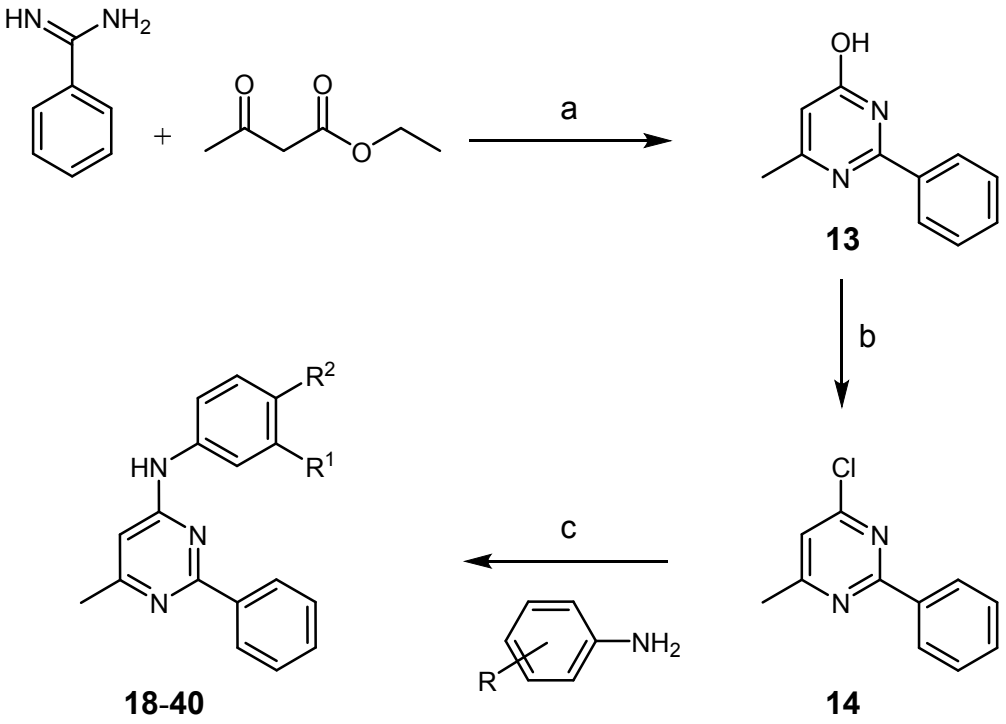

R^1 = **18**, **29**: cyano
19: methyl
21, **32**: nitro
23: hydroxy
24: hydroxymethyl
25, **34**: methoxy
26, **35**: fluoro
27, **33**: chloro
28, **30**: bromo
31, **36**: trifluoromethyl
20, **22**: H

R^2 = **18**, **19**, **30**, **31**: cyano
20: cyanomethyl
22, **33**: nitro
32: fluoro
34: bromo
35, **36**: methoxy
21, **23**-**28**: H

R = **37**: pyridine
38: pyrazine
39: 1,4-dioxane
40: phthalimide

Scheme 1: General synthesis of 4-anilino-6-methyl-2-phenylpyrimidine derivatives. Reagents and conditions: (a) NaOEt/EtOH, reflux, overnight; (b) $POCl_3$ reflux, 8-9 h; (c) *i*-PrOH, microwave, 110°C, 30 min.

Biological Investigation

Inhibitory Activity against ABCG2. The synthesized compounds **18**-**40** were

investigated for their inhibitory activity against ABCG2 using ABCG2-overexpressing MDCK II BCRP cells in Hoechst 33342 and pheophorbide A assays. In short, blockage in both cases results in enhanced intracellular accumulation of these fluorescent ABCG2 substrates. The degree of inhibition of the evaluated compounds correlates with the measured amount of fluorescence. Ko143 [(3S,6S,12aS)-1,2,3,4,6,7,12,12a-octahydro-9-methoxy-6-(2-methylpropyl)-1,4-dioxopyrazino[1′,2′:1,6]pyrido[3,4-b]indole-3-propanoic acid 1,1-dimethylethyl ester; **41**] was chosen as reference compound. The results of the biological investigations are summarized in Table 1. The evaluated compounds were compared to certain pyrimidine analogs reported by *Krapf* et al. as these marked the starting scaffold of the present investigation.[57] The within this work designed and synthesized compounds can be divided into six sub-groups: (i) nitrogen-containing derivatives (**18**-**22**); (ii) oxygen-containing analogs (**23**-**25**); (iii) halogen-containing pyrimidines (**26**-**28**); (iv) nitrogen- and halogen-containing derivatives (**29**-**33**); (v) oxygen- and halogen-containing analogs (**34**-**36**); as well as (vi) pyrimidines with bulky rigid heterocyclic residues (**37**-**40**). Compound **15** represents the unsubstituted pyrimidine derivative which had an IC_{50} value of 0.648 µM in the Hoechst 33342 assay.[57] In earlier studies cyano or nitro substituents had a positive impact on ABCG2 inhibition[61] which could also be shown for the 3-cyano (**16**; $IC_{50\ (Hoechst\ 33342)}$ = 0.122 µM) and 4-cyano (**17**; $IC_{50\ (Hoechst\ 33342)}$ = 0.128 µM) analogs.[57] In sub-group (i), the 3,4-dicyano analog **18** possessed slightly inferior inhibitory activity ($IC_{50\ (Hoechst\ 33342)}$ = 0.188 µM; $IC_{50\ (Pheophorbide\ A)}$ = 0.516 µM). The 3-methyl 4-cyano derivative **19** showed excellent inhibitory power in the Hoechst 33342 assay (IC_{50} =

0.0935) with a maximal inhibition level (I_{max}) value similar to **41**. On the other hand, introduction of a carbon between the main scaffold and the 4-cyano (**20**) led to a major loss of inhibitory power.

The most potent pyrimidine-based ABCG2 inhibitor known until today with its 3-nitro 4-hydroxy substitution pattern had an IC_{50} value of 0.0988 μM (**10**).[57] Investigation of the 3-nitro (**21**) and 4-nitro (**22**) analogs resulted also in very potent inhibitors, the first being as potent as the cyano derivatives **16**-**17**, the latter exceeded the inhibitory potency of compound **10** by a factor of ~2 in the Hoechst 33342 assay (Figure 4 A). Interestingly, in the pheophorbide A assay, both compounds **21** and **22** were equipotent (IC_{50} ≈ 0.150 μM), but with a depressed maximum inhibition level (I_{max}) of < 70%.

Compound set (ii) comprised of pyrimidines with solely oxygen-containing substituents. Here, the 3-hydroxy analog **23** was 2-fold less potent than the cyano derivatives **16**-**17** in the Hoechst 33342. In the pheophorbide A assay, compound **23** was equipotent to the 3,4-dicyano derivative **18**. As already shown for compound **20**, the insertion of a methylene linker at position 3 resulted in a nearly 20-fold loss of inhibitory activity of compound **24** in the Hoechst 33342 assay. On the other hand, the 3-methoxy derivative **25** was equally potent as the 3-hydroxy compound **23**, but with a higher I_{max} value similar to the standard inhibitor **41**.

In group (iii), representatives with solely halogen-containing substituents were synthesized [(3-fluoro (**26**), 3-chloro (**27**), or 3-bromo (**28**)]. These variations resulted in compounds with equal inhibitory activity of around ~1 μM in the Hoechst 33342

assay. Strikingly, compound **28** was ~2-fold more potent compared to compounds **26**-**27** in the pheophorbide A assay (IC_{50} = 0.386 μM).

In the next step, combinations of the above stated substituents were evaluated. Within compound set (iv), compounds **29**-**30** (3-cyano-4-fluoro and 3-bromo-4-cyano, respectively) were found to be the most potent representatives as determined in the pheophorbide A assay, with IC_{50} values in the high double-digit nanomolar concentration range. These data were confirmed in the Hoechst 33342 assay, although the determined IC_{50} values were ~2-3.5-fold higher. However, it must be taken into account that both compounds had depressed I_{max} values in the pheophorbide A assay (59 and 40%, respectively) as shown in Figure 4 B, which artificially decreases the IC_{50} value. This so-called 'partial inhibition' frequently occurs in the literature.[58,61,65,90,91,92,93,94,95] Potential explanations could be reduced solubility or increased intrinsic toxicity of the compounds, but also an actual partial antagonisms against the transporter. The other way around, the 3-trifluoromethyl 4-cyano analog **31** had superior power against ABCG2 in the Hoechst 33342 assay, exceeding the most potent pyrimidine **10** up to now (IC_{50} = 0.0693 μM) and being around 10-fold more potent than the unsubstituted representative **15**. Conversely, inhibition of ABCG2-mediated pheophorbide A transport was over 5-fold weaker. Discrepancies like these occur some times and depend on the manner of fluorescence dye and are influenced by, for example, its polarity, lipophilicity, membrane distribution, velocity of diffusion, affinity to transport protein.[96,97]

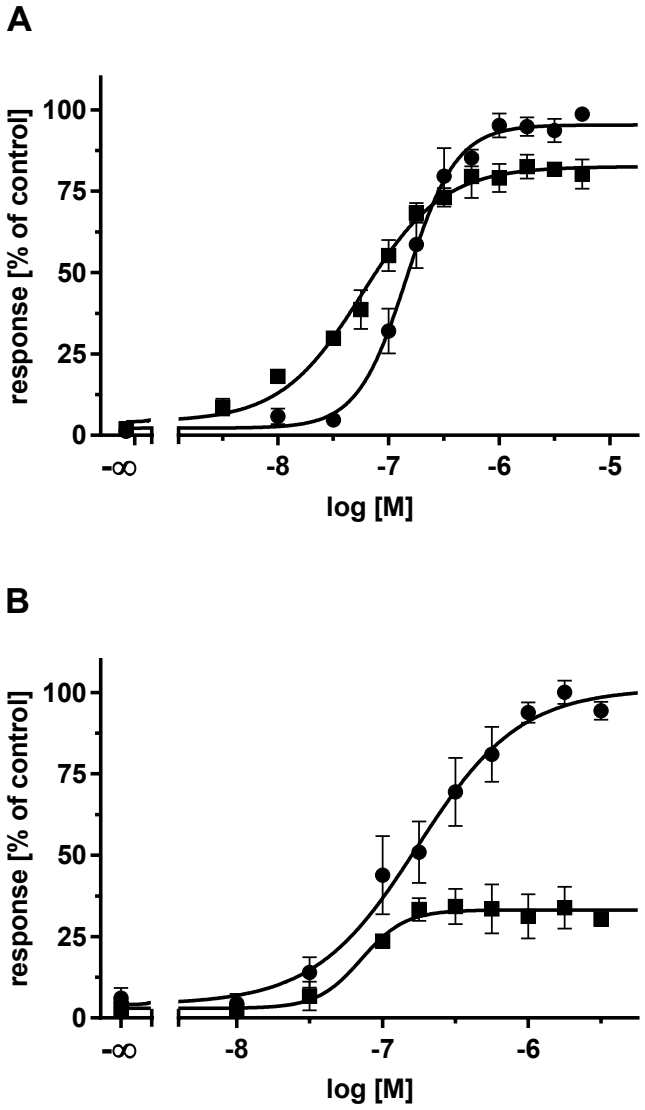

Figure 4: (A) Concentration-effect curves of compound **22** (■, IC_{50} = 0.0522 µM) in comparison to reference inhibitor **41** (●, IC_{50} = 0.220 µM) in the Hoechst 33342 assay. (B) Concentration-effect curves of compound **30** (■, IC_{50} = 0.0594 µM) in comparison to reference inhibitor **41** (●, IC_{50} = 0.274 µM) in the pheophorbide A assay. Shown is mean ± standard error of the mean (SEM) of at least three independent experiments.

Unexpectedly, the 3-nitro 4-fluoro derivative **32** did not result in superior inhibitory power as described for its 3-cyano analog **29.** It was by factors of ~3 and ~9 less active

in the Hoechst 33342 and pheophorbide A assays, respectively. The 3-chloro 4-nitro derivative **33** was the second most potent inhibitor in the Hoechst 33342 assay (IC_{50} = 0.0589 μM), with a notable I_{max} value of above 75%. This could not be confirmed by the pheophorbide A data, as the determined IC_{50} value was ~4-fold higher.

Given the positive impact of methoxy groups in some scaffolds on ABCG2 inhibition,[58,90] certain representatives were synthesized containing either 3- or 4-methoxy and a neighbored halogen in group (v). The 3-methoxy 4-bromo derivative **34** had in both assay an inhibitory power against ABCG2 of ~300 nM but a decreased I_{max} value in the pheophorbide A assay of about 50%. The 4-methoxy derivatives **35** and **36** were less preferred (IC_{50} values of ~1 μM and ~0.5 μM, respectively). Collectively, the methoxy derivatives did not meet the expected results.

In group (vi), heteroaromatic and heterocyclic substituents at positions 3 and 4 of the pyrimidine scaffold were introduced to evaluate rigid nitrogen and oxygen substituents. The pyridine derivative **37** was by a factor of ~2 superior compared to the quinoxaline analog **38** in the pheophorbide A assay. Unfortunately, these compounds could not be evaluated in the Hoechst 33342 assay due to auto-fluorescence. The non-aromatic oxygen analog to compound **38**, the 1,4-dioxane **39**, was inferior to its aromatic nitrogen counterpart, which might be due to loss of planarity and/or aromaticity. The phthalimide derivative **40** was inferior to its closed-ring pyrimidine analogs **37**-**39**. Collectively, the results concerning these compounds showed that a certain flexibility of the substituents is needed for good inhibitory activity.

Table 1: Inhibitory potencies of synthesized pyrimidine derivatives as obtained in the Hoechst 33342 and pheophorbide A assays, respectively, using ABCG2-overexpressing MDCK II BCRP cells. Data are expressed as mean ± SEM (n ≥ 3).

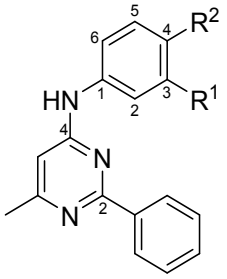

18-**40**

No.	R_1	R_2	Hoechst 33342		pheophorbide A	
			IC_{50} ± SEM [μM]	I_{max} ± SEM [%]	IC_{50} ± SEM [μM]	I_{max} ± SEM [%]
10[b]	NO_2	OH	0.0988 ± 0.0174	n.t.	n.t.	n.t.
15[b]	H	H	0.648 ± 0.085	n.t.	n.t.	n.t.
16[b]	CN	H	0.122 ± 0.014	n.t.	n.t.	n.t.
17[b]	H	CN	0.128 ± 0.018	n.t.	n.t.	n.t.
18	CN	CN	0.188 ± 0.010	117 ± 10	0.548 ± 0.043	100[a]
19	CH_3	CN	0.0935 ± 0.0183	106 ± 11	0.175 ± 0.011	76 ± 12
20	H	CH_2CN	2.50 ± 0.19	100[a]	3.62 ± 0.27	100[a]
21	NO_2	H	0.130 ± 0.011	80 ± 5	0.146 ± 0.009	68 ± 6
22	H	NO_2	0.0522 ± 0.0037	79 ± 5	0.156 ± 0.016	67 ± 10
23	OH	H	0.253 ± 0.027	74 ± 8	0.516 ± 0.033	59 ± 3

24	CH_2OH	H	4.22 ± 0.36	100[a]	2.52 ± 0.12	100[a]
25	OCH_3	H	0.271 ± 0.061	96 ± 6	0.503 ± 0.046	100[a]
26	F	H	1.11 ± 0.15	100[a]	0.776 ± 0.151	100 [a]
27	Cl	H	0.811 ± 0.081	100[a]	1.00 ± 0.18	100 [a]
28	Br	H	0.892 ± 0.091	100[a]	0.386 ± 0.046	83 ± 3
29	CN	F	0.307 ± 0.007	100[a]	0.0861 ± 0.0043	59 ± 6
30	Br	CN	0.119 ± 0.006	90 ± 6	0.0594 ± 0.0036	40 ± 5
31	CF_3	CN	0.0693 ± 0.0009	114 ± 7	0.385 ± 0.047	92 ± 4
32	NO_2	F	1.01 ± 0.12	100[a]	0.771 ± 0.086	100[a]
33	Cl	NO_2	0.0589 ± 0.0015	76 ± 9	0.228 ± 0.025	86 ± 9
34	OCH_3	Br	0.280 ± 0.042	100[a]	0.328 ± 0.031	53 ± 3
35	F	OCH_3	0.861 ± 0.053	100[a]	1.31 ± 0.10	100[a]
36	CF_3	OCH_3	0.598 ± 0.075	100[a]	0.544 ± 0.035	83 ± 5
37			n.t.[c]	n.t.[c]	0.151 ± 0.014	79 ± 16
38			n.t.[c]	n.t.[c]	0.312 ± 0.045	100[a]
49	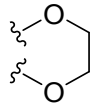		0.808 ± 0.050	100[a]	1.63 ± 0.17	100[a]
40	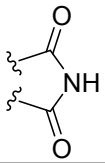		0.253 ± 0.007	105 ± 7	0.416 ± 0.043	101 ± 15
41			0.220 ± 0.006	100	0.274 ± 0.014	100

n.t. = not tested

[a] Constrained to **41**.

[b] Data taken from reference [57].

[c] Data could not be analyzed due to auto-fluorescence of compound at wavelength 355 nm.

Screening against ABCB1 and ABCC1. All compounds were examined for their inhibitory power against ABCB1 and ABCC1 in order to investigate their selectivity over ABCG2 and to potentially discover multi-target ABCB1/ABCC1/ABCG2 inhibitors. The screening was performed at a concentration of 10 µM using a calcein AM assay with either ABCB1-overexpressing A2780/ADR or ABCC1-overexpressing MDCKII MRP1 cells. In short, inhibition of the transporter(s) results in enhanced persistence of calcein AM inside the cell, which becomes cleaved by unspecific esterases to fluorescent calcein. As already stated above for the Hoechst 33342 and pheophorbide A assays, the amount of measured fluorescence correlates to the degree of inhibition exerted by the compounds. Cyclosporine A (10 µM) was used as a positive control. Figure 5 A gives the results of the screening against ABCB1, while Figure 5 B depicts the results regarding ABCC1.

Several pyrimidines, especially representatives with methoxy substituents (**25**), halogen residues (**26**-**28**), or a combination of both substituents (**34**-**36**) had an inhibitory effect on ABCB1 and ABCC1. On the other hand, derivatives with cyano (**18**, **19**, **29**-**31**) and nitro (**21**-**22**,**32**-**33**) groups inhibited neither ABCB1 nor ABCC1 besides few exceptions (**21**-**22**). Compounds with an inhibition level of at least 25% were further

evaluated for their IC_{50} value and the results are presented in Table 2. Generally, these compounds had similar inhibitory potencies against both transporters. The most potent ABCG2 inhibitors (**19**, **29**, **31**, **33**) were ABCG2-selective without noticeable affinity to the other two ABC transporters. Exceptions were compounds **21** and **22**. The former also slightly inhibited ABCC1, which made it (a rather ABCG2-seletive) dual ABCC1/ABCG2 inhibitor. The latter inhibited both ABCB1 and ABCG2, but also with great preference for ABCG2. Nevertheless, compound **22** can be considered as rare finding of a triple ABCB1/ABCC1/ABCG2 inhibitor. In addition, compounds **25**, **27**-**28**, **34**-**38, and 40** were also found to be multi-target ABCB1/ABCC1/ABCG2 inhibitors, which is extraordinary considering the amount of less than 120 compounds of this kind given in literature. Five of the herein presented compounds (**27**-**28**, **34**, **36**-**37**) had potencies ranging within the 50 most potent triple ABCB1/AABCC1/ABCG2 inhibitors known until today.[38,49,54,55,61,62,63,64,65,66,74,75,76,77,78,79,80,81,82,83,84]

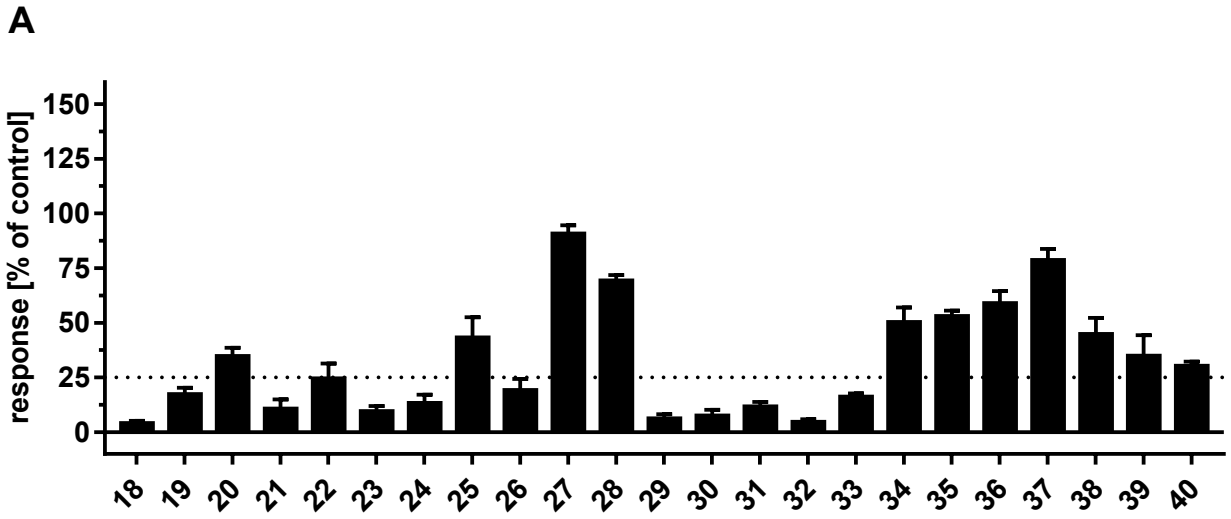

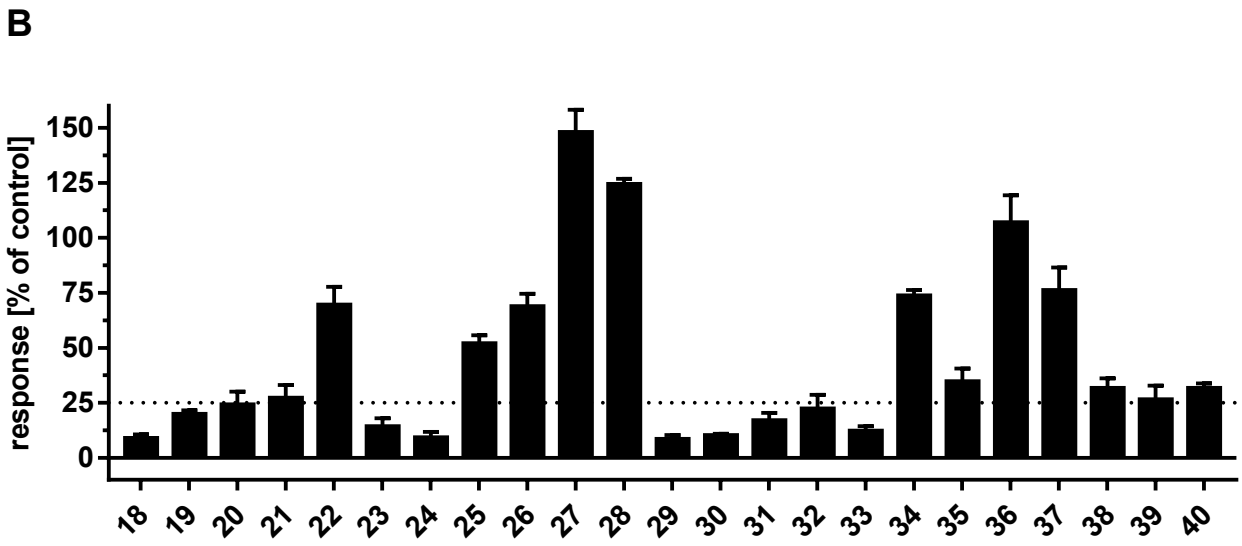

Figure 5: Inhibitory effect of screened compounds at 10 µM against ABCB1 using the ABCB1-overexpressing cell line A2780/ADR (A) and ABCC1 using the ABCC1-overexpressing cell line MDCK II MRP1 (B) applying a calcein AM assay. Data were normalized by defining the effect of 10 µM cyclosporine A as positive control (100%) and buffer medium as negative control (0%). Shown is mean ± SEM of at least three independent experiments with duplicate measurements.

Table 2: Inhibitory potencies against ABCB1 and ABCC1 of compounds that had an inhibition level of at least 25% in the initial screening. Data were obtained in a calcein AM assay using A2780/ADR and MDCK II MRP1. Maximum inhibition was defined by 10 µM of cyclosporine A. Shown is mean ± SEM of at least three independent experiments.

Compound	IC_{50} [μM] ± SEM A2780/ADR (ABCB1)	IC_{50} [μM] ± SEM MDCK II MRP1 (ABCC1)
20	16.0 ± 1.6	n. t.
21	n. t.	11.2 ± 2.8
22	11.2 ± 2.7	9.26 ± 0.75
25	13.4 ± 0.6	8.87 ± 1.00
26	n. t.	7.01 ± 1.01
27	5.92 ± 0.14	3.51 ± 0.05
28	7.14 ± 0.33	3.53 ± 0.06
34	5.03 ± 0.59	6.13 ± 0.37
35	8.99 ± 0.55	19.5 ± 4.7
36	7.30 ± 0.23	4.76 ± 0.72
37	5.13 ± 0.20	7.23 ± 0.69
38	13.4 ± 2.7	28.4 ± 5.0
39	13.1 ± 1.5	30.4 ± 11.0
40	17.7 ± 3.6	18.3 ± 1.2
Cyclosporine A	1.20 ± 0.03	6.63 ± 0.67

n. t. = not tested due to lack of activity in initial screening assay.

Determination of the Concentration-dependent Reversal of ABCG2-mediated MDR. The ability of the most potent compounds to reverse ABCG2-mediated MDR was verified by a MTT-based approach, using a dilution series of the ABCG2 substrate **4**.

In addition, certain concentrations of the tested compounds were added to evaluate whether toxicity of compound **4** was enhanced by presence of the tested compounds (Figure 6 A). This would be indicated by the shift of the concentration-effect curve to the left (closer to the curve of the parental cell line without ABCG2 expression), which means that less compound **4** is necessary for half-maximal growth inhibition due to the presence of the tested compound. This effect can be quantified by plotting the resistance factors of the different experiments as well as the parental cell line against the concentration of the tested compound. This half-maximal reversal concentration (EC_{50}) is the concentration at which the cancer cells were half-maximally sensitized with respect to compound **4** and is comparable to IC_{50} values in the inhibition assays (Figure 6 B).

All chosen compounds were able to achieve full MDR reversal. Their EC_{50} values were in the low double-digit nanomolar concentration range (Table 3), which gave proof that pyrimidines are very effective reversers of ABCG2-mediated MDR. The most efficient MDR reverser was compound **19**, which was able to sensitize MDCK II BCRP cells with an EC_{50} value of 11.0 nM (Figure 6 A and B). This exceeds the efficacy of its parent compound **9**[56] and makes it one of the most potent MDR reversers reported until today.[56,57,89] In addition, this EC_{50} value is of a 6- and 12- fold higher potency compared to the results of the Hoechst 33342 or pheophorbide A assays, respectively. This phenomenon can be explained by different affinities of the ABCG2 substrates for the transporter and transport behavior of the different substrates.[96,97] It might also be

correlated to the different time frames of the assays (short-term vs. long-term), and has already been observed in literature before.[65,90]

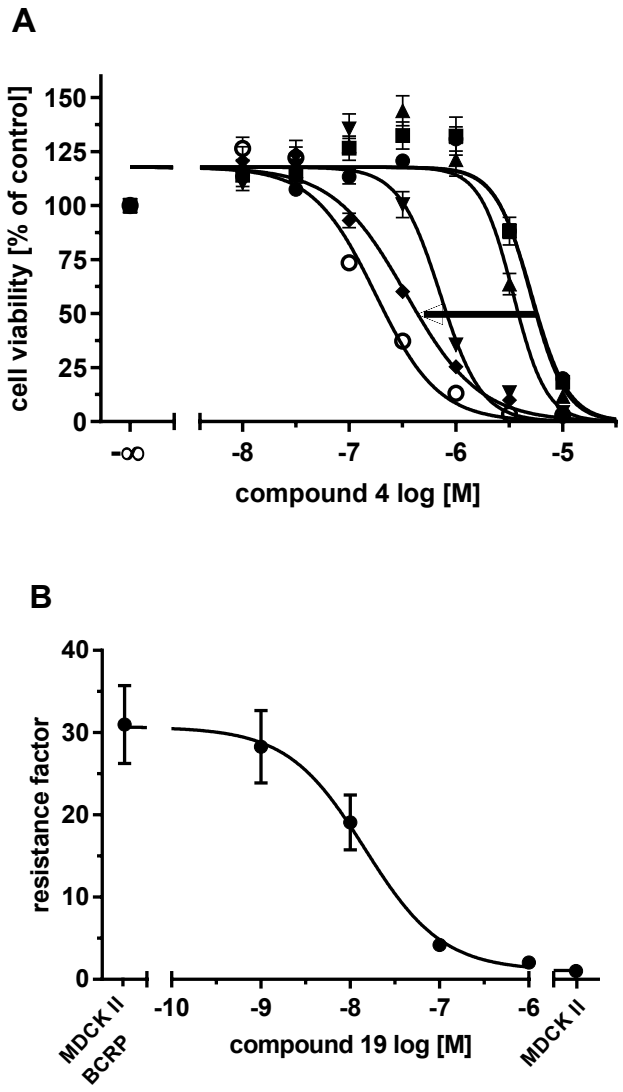

Figure 6: (A) MDR reversal assay obtained in a MTT-based cell viability assay for compound **19**. The curve shows sensitization of ABCG2-overexpressing MDCK II BCRP cells with regard to compound **4**. Compound **19** was used at concentrations of 0 μM (●), 0.001 μM (■), 0.010 μM (▲), 0.100 μM (▼), and 1.000 μM (♦) and was compared to the wild type cell line without compound addition (○). Shown is mean ±

SEM of at least three independent experiments with duplicate measurements. (B) Calculated resistance factors derived from GI_{50} values of graph (A) were plotted against the used concentrations of compound **19**. A nonlinear regression of the obtained curve yielded a half-maximal sensitization concentration (EC_{50}) of 11 nM. Shown is mean ± SEM of at least three independent experiments.

Table 3: Results of the MDR reversal assay obtained in a MTT-based viability assay. Resistance factors were plotted against the corresponding concentration of the investigated compound. The nonlinear regression of the obtained curve gave the half-maximal reversal concentration (EC_{50}). Shown is mean ± SEM.

Compound	EC_{50} [μM] ± SEM
19	0.0110 ± 0.0015
22	0.0159 ± 0.0009
29	0.0209 ± 0.0005
30	0.0150 ± 0.0020
31	0.0152 ± 0.0016

Determination of the Time-dependent Reversal of ABCG2-mediated MDR. In order to investigate the MDR reversing property of the most potent representative – compound **19** – in more detail, a time-dependent MTT-based MDR reversal assay was conducted. In short, cells were exposed to a concentration of 0.5 μM of compound **4** alone and in

combination with 10 nM of compound **19** over a time period of seven days determining the cell viability every day. These concentrations were chosen as 0.5 µM of compound **4** showed in preliminary experiments no toxic effect on the resistant cells over 3 days, and 10 nM of compound **19** nearly equals its EC_{50} value. Figures 7 A [normalized on control (pure cell culture medium)] and B (normalized on compound **4**) show the obtained results. As one can see, 10 nM of compound **19** is sufficient to double the toxic effect of compound **4** over a period of 7 days. A statistically significant effect was seen after 5 days, which equals the timeline of a commonly used application in antineoplastic chemotherapy (so-called 5-day-course; 5 days topotecan i.v. application every 3 weeks).[98] To verify the concentration-dependency of this effect over time, this 7-days-experiment was conducted using different concentrations of compound **19** (0, 10, 25, and 50 nM). Figure 7 C presents the obtained results, showing that increased concentrations of compound **19** led to decreased cell viability over time. Plotting the inflection points of the curves of Figure 7 C against the used concentrations of compound **19** results in a time-concentration graphic as indicated by Figure 7 D. Several measures can be deduced from this plot: (i) t_{max}, which represents the time needed for the antineoplastic agent alone at a fixed concentration (in this case compound **4** at 0.5 µM) to half-maximally kill the cancer cells (~7.25 days); (ii) t_{min}, which represents the minimum time needed to achieve half-maximal cell death by the antineoplastic agent at a fixed concentration in combination with a sensitizer (in this case compound **19**; ~4.25 days); (iii) c_{tmin} (maximal cell death acceleration concentration), which is the concentration of the modulator needed to achieve t_{min} (in

this case compound **19** at ~50 nM); and (iv) $c_{½tmax}$ (half-maximal cell death acceleration concentration), which gives the concentration of the modulator needed to achieve half-maximal cell death by the used antineoplastic agent at ½ of t_{max} (in this case compound **19** at 17.26 nM in ~5.75 days in combination with compound **4** at 0.5 µM; Figure 8 D). $c_{½tmax}$ is a compound-, cell line-, antineoplastic agent-, and assay-specific value, which is described for the first time within this work. It is a critical measure for judging the effectiveness of a modulator and its superiority to the treatment with an antineoplastic agent alone, especially regarding its relation over time. Besides IC_{50} (relation to target) and EC_{50} (capability to reverse MDR), $c_{½tmax}$ should be the third standard measure in future compound evaluation.

In summary, it can be stated that compound **19** (i) half-maximally sensitizes ABCG2-overexpressing cells at only 11 nM in combination with varying concentrations of compound **4**; (ii) sensitizes ABCG2-overexpressing cells in combination with 0.5 µM compound **4** two times as effective as compound **4** does alone; and (iii) accelerates cell death half-maximally at ~17.25 nM considering treatment with compound **4** alone and the maximal possible acceleration of cell death represented by use of ~50 nM of compound **19**. In essence, this makes compound **19** most potent sensitizer of ABCG2-mediated MDR in detail.

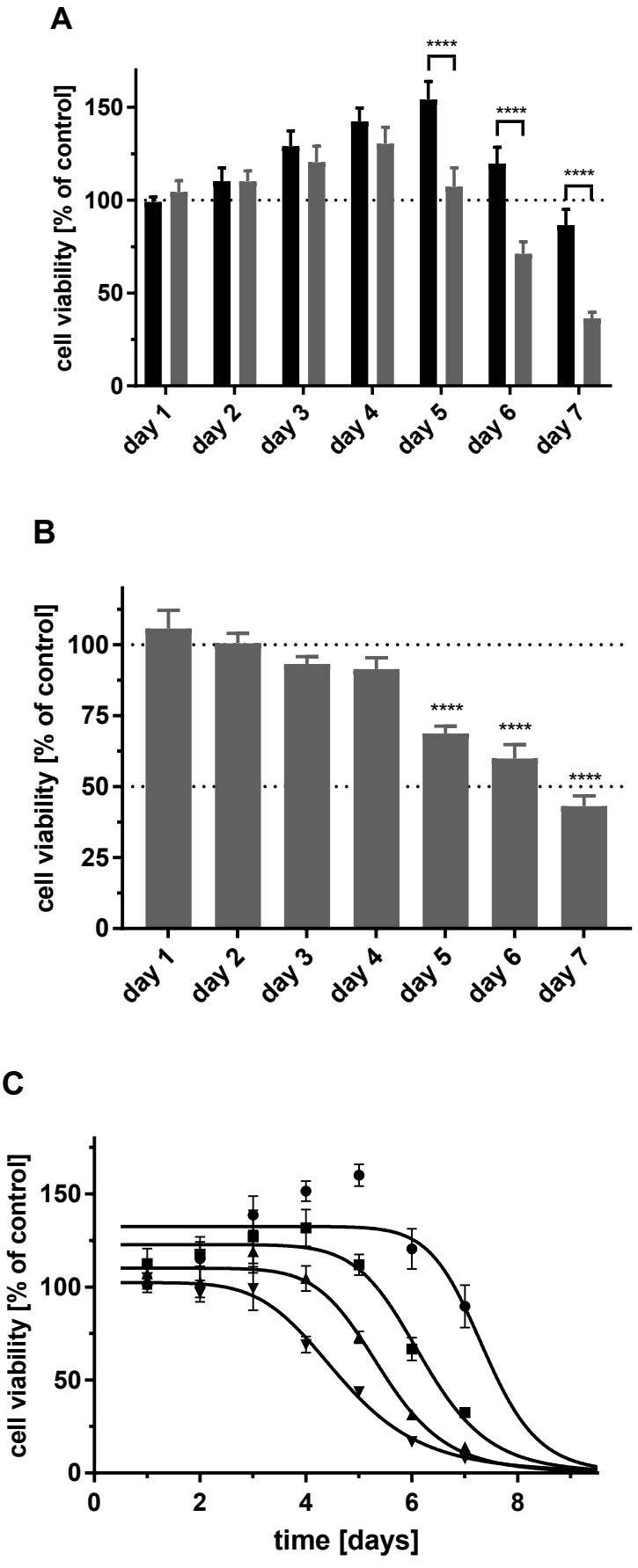
A
cell viability [% of control]
150
100
50
0
****
****
****
day 1
day 2
day 3
day 4
day 5
day 6
day 7
B
cell viability [% of control]
100
75
50
25
0
****
****
****
day 1
day 2
day 3
day 4
day 5
day 6
day 7
C
cell viability [% of control]
150
100
50
0
0
2
4
6
8
time [days]

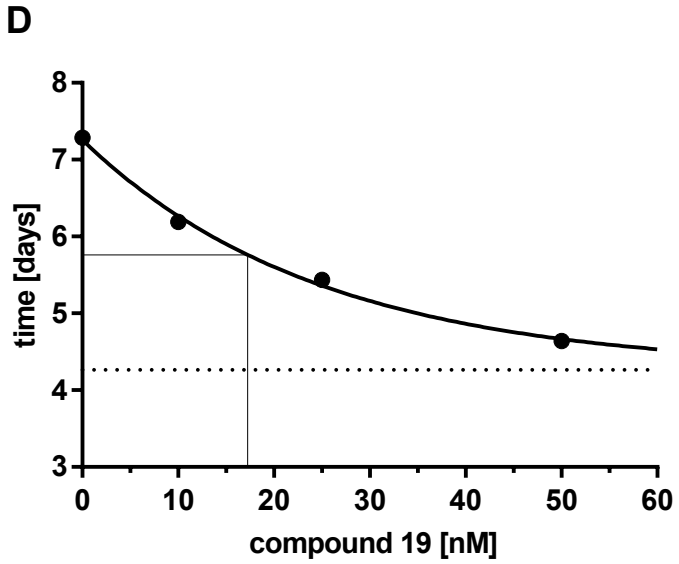

Figure 7: Time-dependent MDR reversal assay using a MTT-based approach. (A-B) Compound **19** was used at a concentration of 10 nM and was combined with 0.5 µM compound **4** over a period of 7 days. Shown is mean ± SEM of at least three independent experiments with triplicate measurements. (A) Normalization was conducted on the effect-value of cells in pure cell culture medium without addition of compound **4** and/or compound **19**. (B) Normalization was conducted on the effect-value of compound **4** alone at the corresponding day. Significance was calculated applying multiple *t*-test and is given as *: $p \leq 0.05$, **: $p \leq 0.01$, ***: $p \leq 0.001$, **** $p \leq 0.0001$. (C) Cell viability-versus-time assay using 0.5 µM of compound **4** and 0 nM (●), 10 nM (■), 25 nM (▲), 50 nM (▼) of compound **19**. Shown is mean ± SEM of at least three independent experiments with triplicate measurements. (D) The inflection points derived from the curves in graphic (C) have been plotted against the used concentration of compound **19**. Nonlinear regression revealed that using 0.5 µM compound **4** in combination with compound **19** the latter is able to accelerate half-

maximal cell death by a factor of 1.7 (~4.25 days vs. ~7.25 days). The half-maximal cell death acceleration concentration of compound **19** was ~17.25 nM.

Evaluation of Multi-target ABCB1, ABCC1, and ABCG2 Inhibitors for Reversal of ABCB1-, ABCC1-, and ABCG2-mediated MDR. The five most potent triple ABCB1/ABCC1/ABCG2 inhibitors as indicated by Tables 1 and 2 – compounds **27**, **28**, **34**, **36**, and **37** – were investigated for their ability to reverse ABCB1-, ABCC1-, and ABCG2-mediated MDR. While the first 4 compounds failed to sensitize ABCB1- and ABCC1-overexpressing cells regarding doxorubicin (data not shown), compound **37** revealed to be a potent, broad-spectrum reverser of ABCB1-, ABCC1-, and ABCG2-mediated MDR. It half-maximally sensitized A2780/ADR (ABCB1), MDCK II MRP1 (ABCC1), and MCDK II BCRP (ABCG2) cells at 8.41 ± 0.48 μM, 5.15 ± 0.68 μM, and 0.0164 ± 0.0023 μM, respectively (Figures 8 A–F). These results make compound **37** a rare example of a triple ABCB1/ABCC1/ABCG2 inhibitor that reversed ABCB1-, ABCC1-, and ABCG2-mediated MDR, which has only been shown for compounds **11** and **12** in the literature before (Figure 3).[65,66]

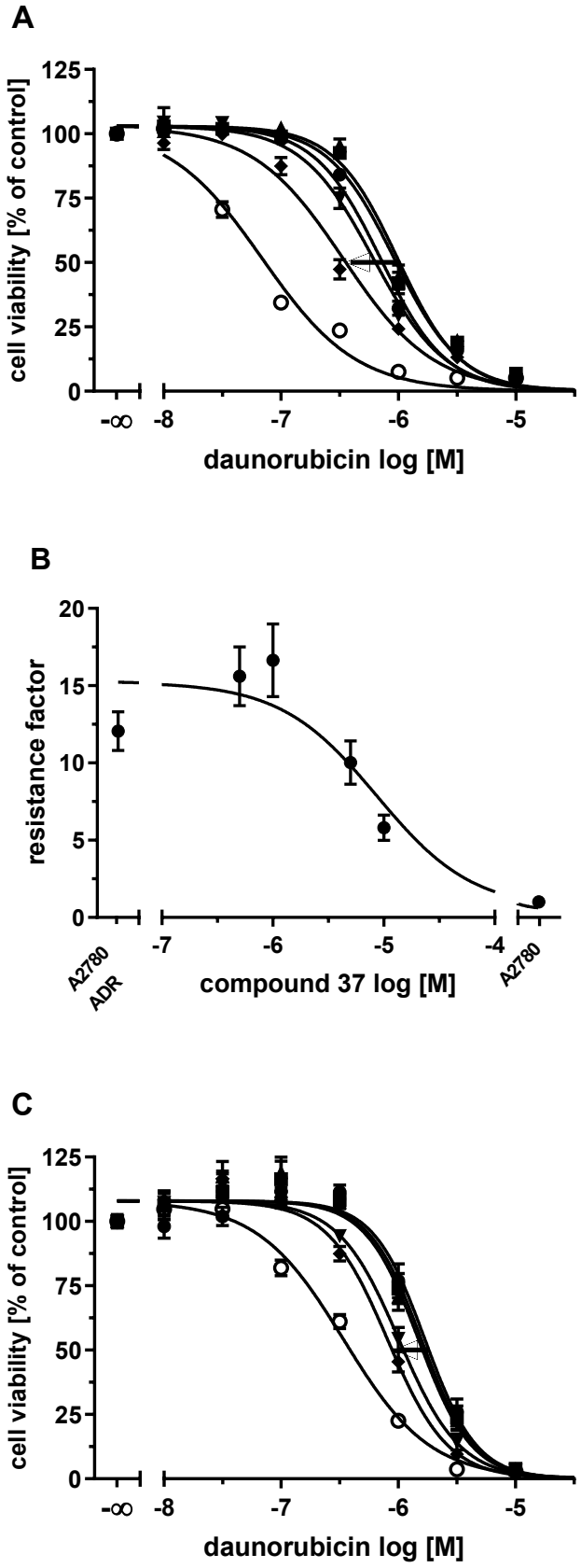
A
cell viability [% of control]
125
100
75
50
25
0
-∞
-8
-7
-6
-5
daunorubicin log [M]
B
resistance factor
20
15
10
5
0
-7
-6
-5
-4
A2780 ADR
compound 37 log [M]
A2780
C
cell viability [% of control]
125
100
75
50
25
0
-∞
-8
-7
-6
-5
daunorubicin log [M]

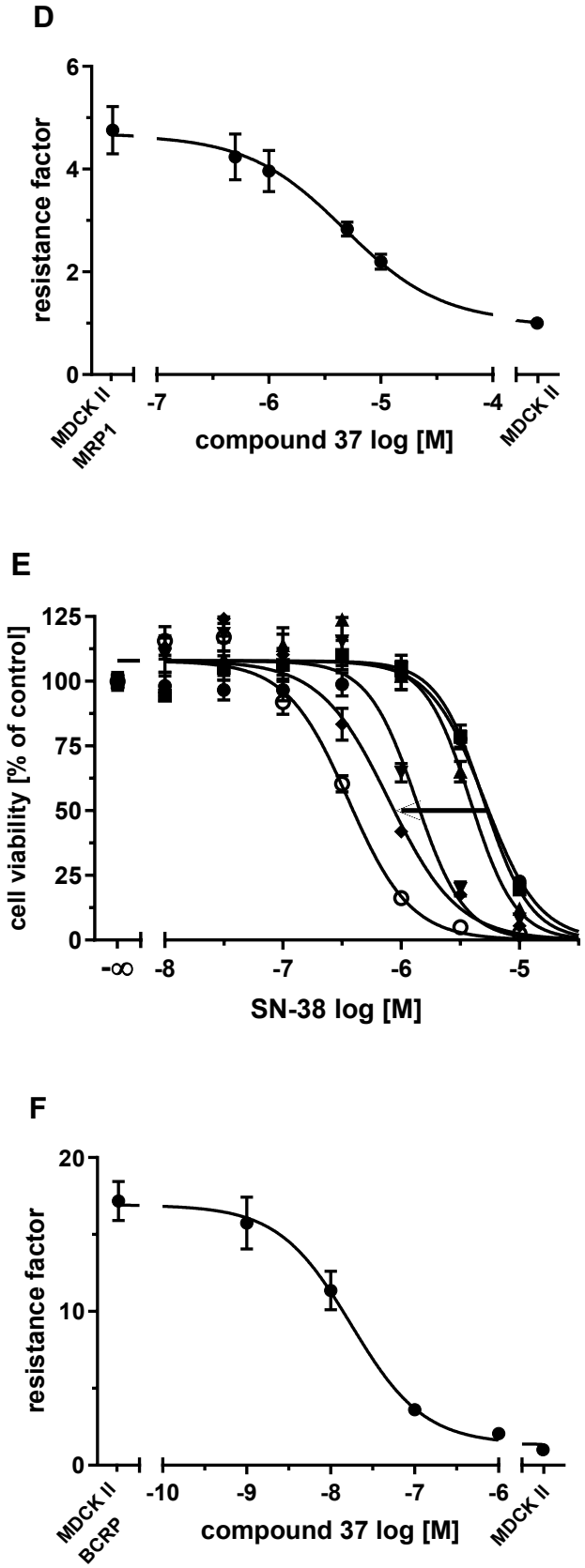
D
resistance factor
6
4
2
0
MDCK II
MRP1
-7
-6
-5
-4
MDCK II
compound 37 log [M]
E
cell viability [% of control]
125
100
75
50
25
0
-∞
-8
-7
-6
-5
SN-38 log [M]
F
resistance factor
20
10
0
MDCK II
BCRP
-10
-9
-8
-7
-6
MDCK II
compound 37 log [M]

Figure 8: (A) Sensitization of ABCB1-overexpressing A2780/ADR cells against daunorubicin by compound **37** at concentrations of 0 μM (●), 0.5 μM (■), 1.0 μM (▲), 5.0 μM (▼), and 10 μM (♦) compared to the wild type cell line A2780 (○). (B) Resulting resistance factors derived from GI_{50} values of graph (A) were plotted against the used concentrations of compound **37**. A nonlinear regression of the obtained curve yielded the half-maximal sensitization concentration (EC_{50}) of 8.41 μM. (C) Sensitization of ABCC1-overexpressing MDCK II MRP1 cells against daunorubicin by compound **37** at concentrations of 0 μM (●), 0.5 μM (■), 1.0 μM (▲), 5.0 μM (▼), and 10 μM (♦) compared to the wild type cell line MDCK II (○). (D) Resulting resistance factors derived from GI_{50} of graph (C) were plotted against the used concentrations of compound **37**. A nonlinear regression of the obtained curve yielded the half-maximal sensitization concentration (EC_{50}) of 5.15 μM. (E) Sensitization of ABCG2-overexpressing MDCK II BCRP cells against compound **4** by compound **37** at concentrations of 0 μM (●), 0.001 μM (■), 0.010 μM (▲), 0.100 μM (▼), and 1.000 μM (♦) compared to the wild type cell line MDCK II (○). (F) Resulting resistance factors derived from GI_{50} of graph (E) were plotted against the used concentrations of compound **37**. A nonlinear regression of the obtained curve yielded the half-maximal sensitization concentration (EC_{50}) of 0.0164 μM. In all cases the mean ± SEM of at least three independent experiments with duplicate measurements is shown.

Determination of the Intrinsic Cytotoxicity Using ABCG2-overexpressing and Wild Type Cells. To evaluate the cytotoxicity of the compounds, a screening was performed using

ABCG2-overexpressing MDCK II BCRP cells and their parental cell line MDCK II in a MTT-based cell viability assay. For the screening, the highest concentration used in the inhibition assays (10 μM) was chosen and the cell viability was compared to pure culture medium as negative control (100%) and 10% DMSO as positive control (0%). The bar chart in Figure 9 shows that the compounds demonstrated no cytotoxicity at this concentration except for compounds **31** and **36**, which might be attributed to the trifluoromethyl substituent. These compounds as well as the most potent reversers of ABCG2-mediated MDR (**19**, **22**, **29**-**30**) were tested for their half-maximal growth inhibition values (GI_{50}), which are summarized in Table 3. While compounds **31** and **36** had GI_{50} values of 9.57 μM and 8.4 μM, respectively, the other evaluated compounds were less toxic (GI_{50} > 15 μM). This was reflected in their therapeutic ratio [$GI_{50\ (resistant\ cell\ line)}$ divided by $IC_{50\ (Hoechst\ 33342\ or\ pheophorbide\ A)}$], which was in many cases greater than 100. Compounds **21** and **29** possessed the highest therapeutic ratios, but it must be considered that the concentration-effect curves of those representatives did not achieve full inhibition in the Hoechst 33342 and pheophorbide A assays, respectively. In this regard, their IC_{50} values are overrated and artificially increased the therapeutic ratios. Figure 10 gives the concentration-effect curves of compounds **29** (nontoxic) and **36** (toxic). All evaluated compounds exhibited no difference in intrinsic toxicity between transfected and wild type cells which leads us to believe that they are not transported.

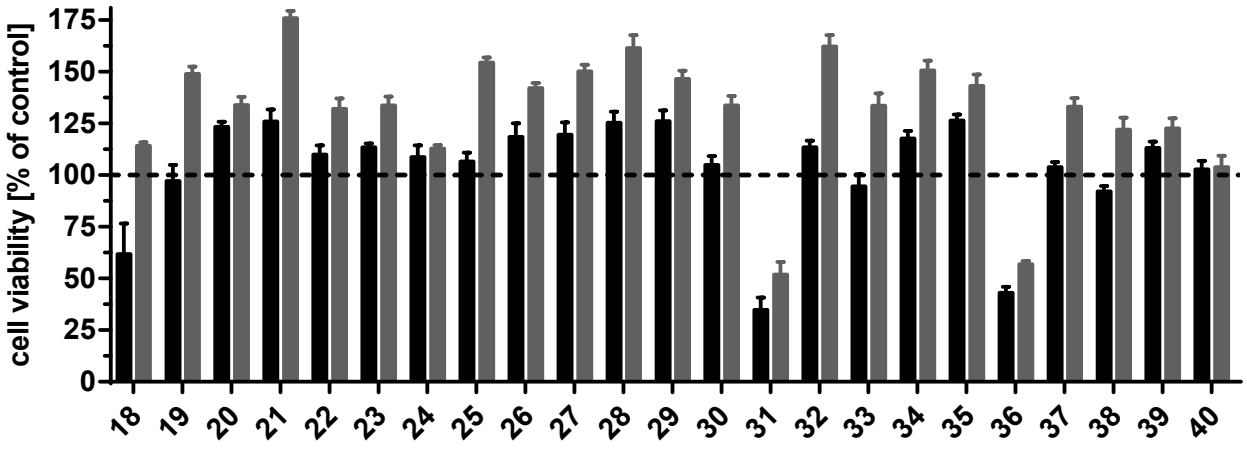

Figure 9: Bar chart showing the influence of the studied compounds (10 µM) on the cell viability of MDCK II BCRP (black) and MDCK II wild type (grey) cells. The data were obtained by a MTT-based assay defining culture medium as negative control (100%) and 10% DMSO as positive control (0%). Shown is mean ± SEM of at least three independent experiments with duplicate measurements.

Table 4: Half-maximal growth inhibition values (GI_{50}) of selected pyrimidines. Shown is mean ± SEM of at least three independent experiments with duplicate measurements. Therapeutic ratio was calculated as the ratio of GI_{50} and IC_{50} values of the resistant cell line and different accumulation assays, respectively.

Compound	GI_{50} (MDCK II BCRP) [µM] ± SEM	GI_{50} (MDCK II wild-type) [µM] ± SEM	therapeutic ratio (tr)	
			Hoechst 33342	pheophorbide A
19	15.7 ± 0.3	15.7 ± 0.6	167	90
22	17.0 ± 0.2	16.7 ± 0.3	327	111

29	96.7 ± 3.5	102 ± 5	315	1122
30	145 ± 36	188 ± 58	1218	2441
31	9.57 ± 0.12	9.89 ± 0.04	139	25
36	8.40 ± 0.35	10.1 ± 2.1	14	15
DMSO	137 ± 4	123 ± 29		

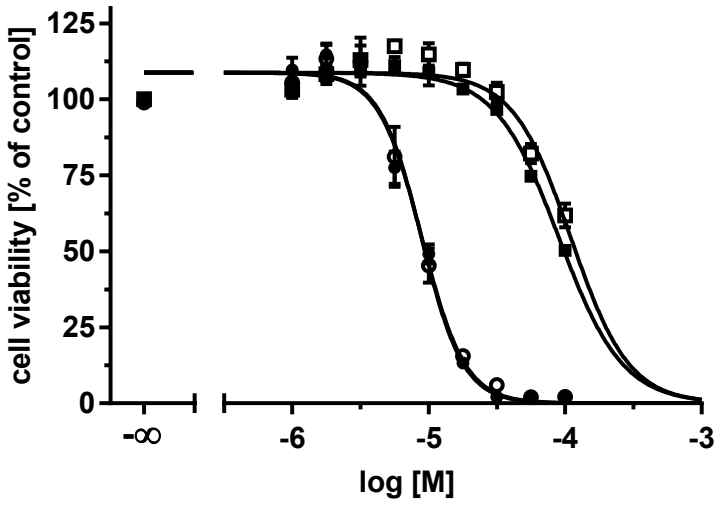

Figure 10: MTT-based viability assays of compounds **29** (■) and **36** (●) using the MDCK II BCRP (closed) and wild type (open) cells. DMSO and culture medium were used to define 0 and 100%, respectively. Shown is mean ± SEM of at least three independent experiments with duplicate measurements.

*Determination of the Intrinsic Cytotoxicity of Compound **37** Using ABCB1-, ABCC1- and ABCG2-overexpressing and Corresponding Wild Type Cells.* The only representative of a potent triple ABCB1/ABCC1/ABCG2 inhibitor and effective reverser of ABCB1-, ABCC1-, and ABCG2-mediated MDR, compound **37**, was evaluated with

respect to its intrinsic toxicity applying the very same cell lines as used in the inhibition assays. Pyrimidine **37** showed almost no toxicity against A2780/ADR (ABCB1; GI_{50} = 28.9 ± 2.9 µM; tr = 5.6) and A2780 (GI_{50} = 22.6 ± 3.4 µM) cells, the MDCK II MRP1 (ABCC1; GI_{50} = 35.4 ± 2.4; tr = 4.9) and MDCK II (GI_{50} = 38.4 ± 2.2) cell line, as well as MDCK II BCRP (ABCG2; GI_{50} = 42.1 ± 3.6; tr = 279) cells.

Investigation of Compound Accumulation in MCF-7 Breast Cancer Cells. As indicated above, the data obtained in the cell viability assays hinted to the fact that the compounds are not transported by ABCG2. To underpin the hypothesis that the compounds are not substrates of ABCG2, the strong auto-fluorescent, nontoxic pyrimidine **38** was analyzed with confocal laser scanning microscopy. Because of the similarities in excitation and emission wavelengths to the green fluorescent protein (GFP) linked to ABCG2 in the MDCK II BCRP cell line, MCF-7/MX cells (ABCG2-overexpressing) and their parental counterpart MCF-7 were used to perform fluorescence studies. Pheophorbide A has been taken as a reference. From the fluorescence spectrum taken by a BD LS-55 Fluorescence Spectrometer, compound **38** shows an excitation maximum at 370 nm and emission maximum at 495 nm. For the measurement an excitation wavelength of 405 nm and an emission filter of 500-530 nm (compound **38**) and 662-737 nm (pheophorbide A) were chosen. No difference in fluorescence intensity of compound **38** in ABCG2-overexpressing MCF-7/MX (Figure 11 A) and parental MCF-7 (Figure 11 B) cells was observed. In contrast, there is a difference in pheophorbide A fluorescence between resistant (Figure 11 C) and

parental (Figure 11 D) cell lines. The addition of compound **38** to MCF-7/MX cells with pheophorbide A (Figure 11 E) increased accumulation of pheophorbide A inside the cells, although the intensity did not reach the level of the parental MCF-7 cell line. The slightly lower intensity can be explained by the concentration used in the assay (1 µM), which was only two times as high as the IC_{50} value of compound **38**. These studies confirmed that compound **38** was able to inhibit active transport mediated by ABCG2 while being not an ABCG2 substrate. Taking these results and the formerly stated MTT-based cell viability assay results into account, the compound class of pyrimidines seems generally not to be transported by ABCG2.

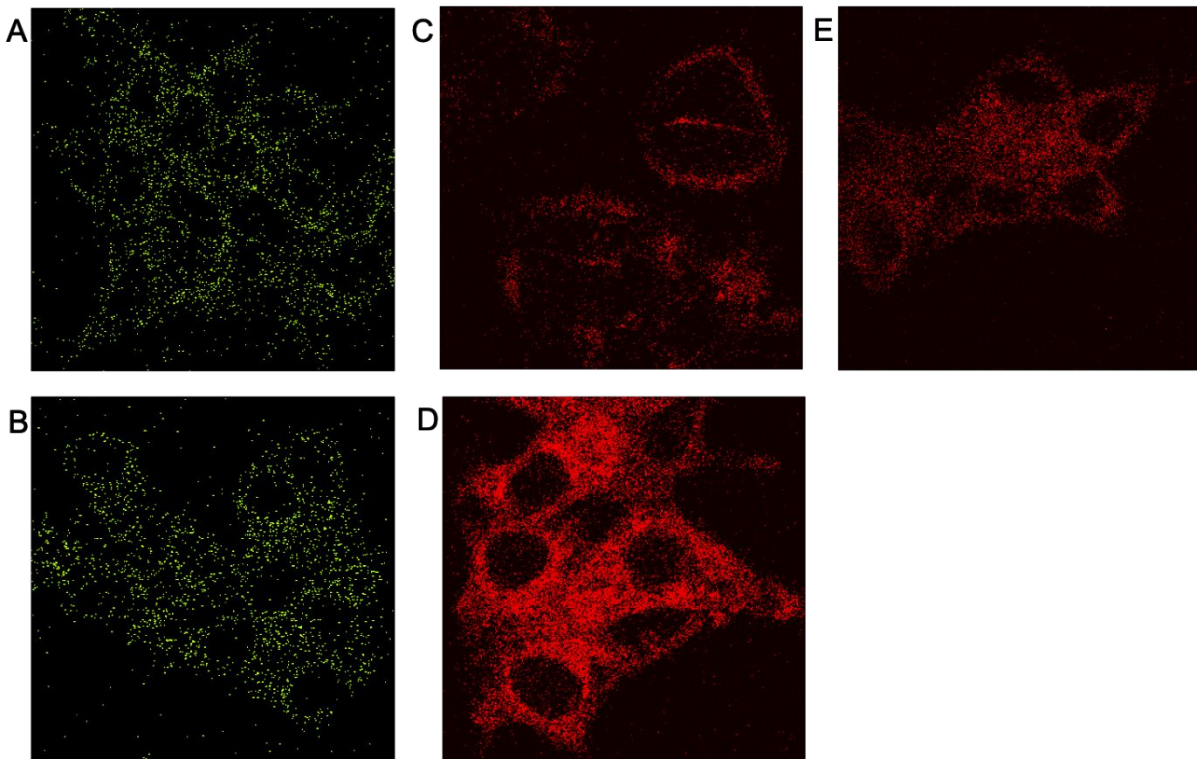

Figure 11: Confocal laser scanning microscopy analysis of accumulation of fluorescent compound **38** (A-B) or (C-D)/and (E) pheophorbide A in ABCG2-overexpressing MCF-

7/MX (A, C, E) or parental MCF-7 (B, D). (A): compound **38** (1 μM) in ABCG2-overexpressing MCF-7/MX cells; (B): compound **38** (1 μM) in parental MCF-7 cells; (C): pheophorbide A (0.5 μM) in ABCG2-overexpressing MCF-7/MX cells; (D): pheophorbide A (0.5 μM) in parental MCF-7 cells; (E): pheophorbide A (0.5 μM) in presence of compound **37** (1 μM) in ABCG2-overexpressing MCF-7/MX cells.

Determination of Mode of Inhibition. The most potent reverser of ABCG2-mediated MDR, compound **19**, was additionally analyzed regarding its mode of inhibition with respect to ABCG2-mediated Hoechst 33342 transport. Lineweaver-Burk analysis resulted in a competitive mode of action (Figure 12 A), which is characterized by an increased K_m value and constant v_{max} value. This interrelationship is also depicted in the Cornish-Bowden plot in Figure 12 B.

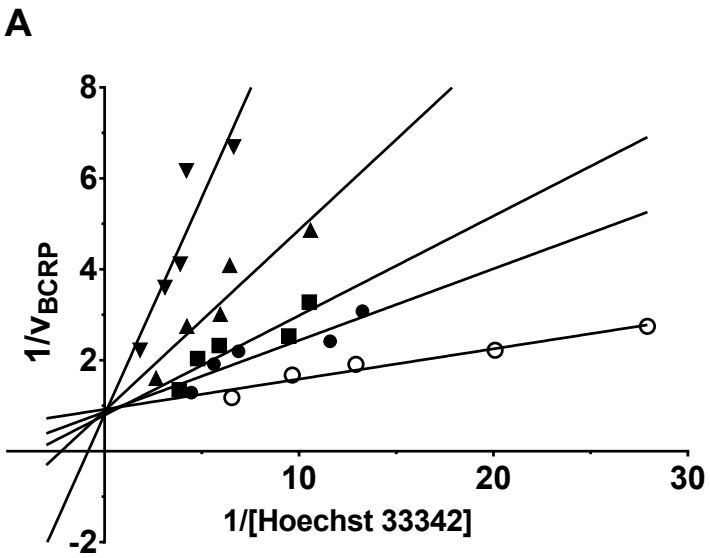

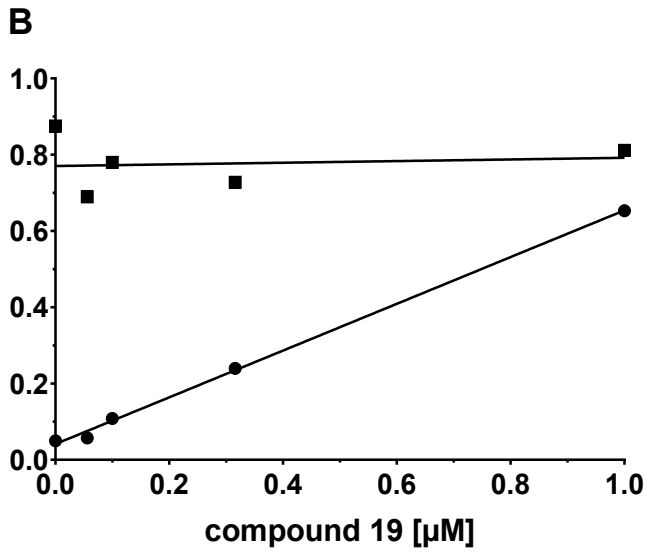

Figure 12: Determination of mode of inhibition by compound **19** using ABCG2-overexpressing MDCK II BCRP cells. (A) Lineweaver-Burk plot of ABCG2-mediated Hoechst 33342 transport at concentrations of 0.3, 0.4, 0.5, 0.6, 0.7, and 1.0 µM. Compound **19** was used at concentrations of 0 µM (○), 0.056 µM (●), 0.100 µM (■), 0.316 µM (▲), and 1.000 µM (▼). (B) Cornish-Bowden plot generated from direct plot of data, in which K_m (●) increases while v_{max} (■) remains the same. Depicted are representative experiments out of three independent experiments.

*Molecular Docking Studies of Compound **19**.* In order to understand the binding mode of compound **19** compared to the substrate Hoechst 33342 and their interaction with ABCG2, we performed molecular modelling studies. The cryo-electron microscopy (cryo-EM) structure of human ABCG2 in complex with the compound **41** analog MZ29 (PDB ID 6FFC) and additional docking studies have recently been reported.[99,100] On this basis we have reported putative binding modes of quinazoline-based ABCG2 inhibitors as well as the ABCG2 substrate Hoechst 33342 and further explained the

mechanism of inhibition of the former.[59] Figure 13 A shows the two binding sites (S1 and S2) of ABCG2 as well as the binding poses of either MZ29 (S1; Figure 13 B)[100] and the proposed binding pose of Hoechst 33342 (S2; Figure 13 C).[59]

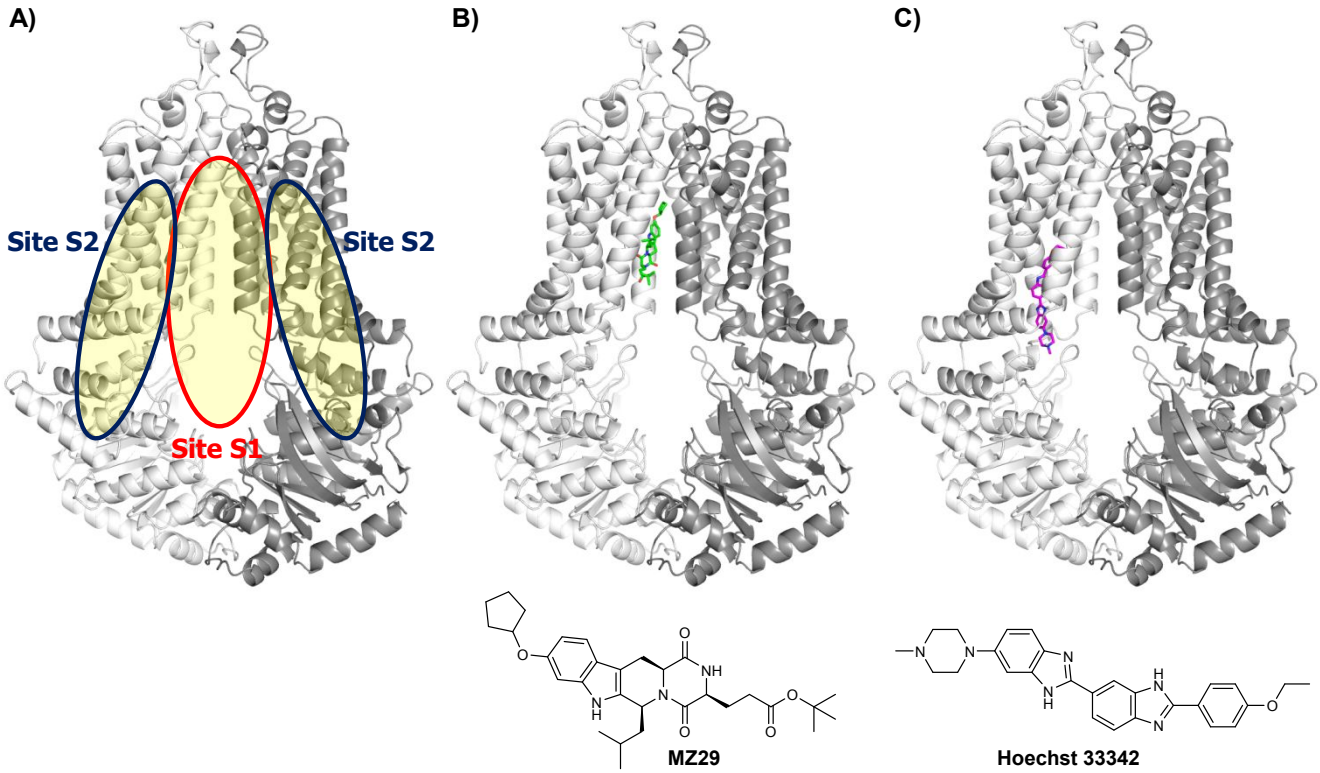

Figure 13: Binding sites (A) and poses of MZ29 (B) and Hoechst 33342 (C) in human ABCG2, which is displayed in cartoon representation (chain A: light gray; chain B: dark gray). Both MZ29 (A) and Hoechst 33342 (B) are shown as stick models. (A) The putative binding sites obtained from the cryo-EM structure of human ABCG2 (PDB 6FFC) are schematically indicated as S1 and S2. (B) The binding pose of MZ29, an analog of compound **41**, (carbon colored green) in the binding pocket of human ABCG2. (C) The docked pose of the ABCG2 substrate Hoechst 33342 (carbon colored magenta)

in the binding pocket of human ABCG2. Oxygen atoms are colored in red and nitrogen atoms in blue.

In this work, we have extended the molecular docking studies to predict the binding pose of compound **19** and explored the binding site as well as prevailing interactions. Among the top 100 binding poses identified from the molecular docking studies using LeadIT, 66% of poses were occupying the binding site S2 in comparison to 34% of poses in S1 (Figure 14 A). The best scoring binding pose of compound **19** is shown in Figure 14 B and the 2D interaction diagram is highlighted in Figure 14 C. The pyrimidine scaffold is positioned in the sub-pocket where the methylpiperazine partial structure of Hoechst 33342 binds. Due to the smaller ring size of the pyrimidine scaffold in comparison to quinazolines, the pyrimidine scaffold binds deeper into the S2 binding site. The phenyl ring substituted at position 2 of the pyrimidine directs into the substrate binding pocket and forms strong hydrophobic interaction with Leu388. The two asparagine residues Asn387 and Asn391 form hydrogen bond interactions with the nitrogen atoms of the pyrimidine scaffold. The 3-methyl 4-cyano phenyl ring substituted at position 4 of the pyrimidine through an amine linker is positioned towards the nucleotide binding domain and located in the sub-pocket formed by a high number of hydrophobic residues Val130, Met131, Gly132, Thr180 and Val450. The 4-cyano group forms a strong electrostatic interaction with Arg191. The amine linker forms a hydrogen bond interaction with Glu451. The hydrogen bond interaction is in agreement with our previous docking and structure-activity relationship studies of quinazolines

which specified that an amine linker is highly important for ABCG2 inhibition.[59] The binding mode and the interaction clearly highlight that compound **19** possibly established a competitive mode of inhibition against the substrate Hoechst 33342 in the S2 binding site of ABCG2 and substantiate the results obtained in the kinetic studies experiments .

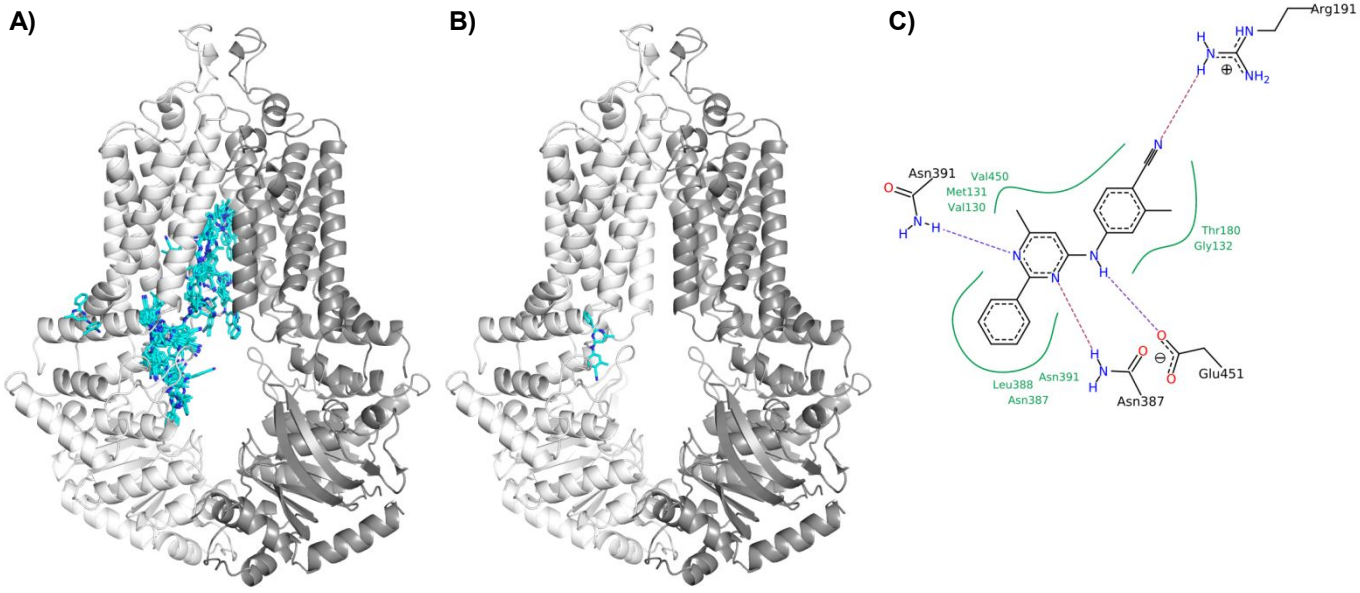

Figure 14: Putative binding poses of compound **19**. (A) The top 100 docked poses of **19** (carbon colored cyan) observed in the cryo-EM structure of human ABCG2 (PDB 6FFC). (B) The best scoring pose of **19** in the S2 binding site. (C) 2D interaction diagram. Oxygen atoms are colored in red and nitrogen atoms in blue.

*Determination of the Influence of Compound **19** on ABCG2 Expression.* Compensatory induction of ABC transporters after chemotherapeutic intervention poses a potential risk for the success of anticancer regimens in general.[19,20,21,22,23,24,25,30,31] Therefore,

compound **19** was evaluated for its capability to interfere with ABCG2 expression to exclude an ABCG2 upregulation. Western blot analysis was performed after cultivation of resistant MDCK II BCRP cells with compound **19** alone and in combination with compound **4** for 4 and 7 days, respectively. These time intervals have been chosen as the MTT-based cell viability assay results given in Figure 7 A indicated a higher cell viability after 4 days when cells were treated with either compound **4** alone or in combination with compound **19**. The 7 days-measurement has been chosen as it marked the end point of the time-dependent MDR reversal assay and equaled in parallel the longest period of exposure to the stated compounds with highest chance of a potential regulatory interference. As can be seen in Figure 15, exposure to compound **4** (0.5 µM) alone led to a 2-fold (day 4) and 5-fold (day 7) upregulation of ABCG2, respectively, which is in agreement with previous reports.[24,25] There was no significant difference in total ABCG2 expression in MDCK II BCRP cells when exposed to compound **4** alone or in combination with compound **19**. The effect of compound **19** alone even showed a contradictory effect as it reduced ABCG2 amount by 36% (day 4; p = 0.0007) and 24% (day 7; not significant). Taken together, compound **19** is not an inducer of ABCG2 and has rather no noteworthy influence on ABCG2 expression.

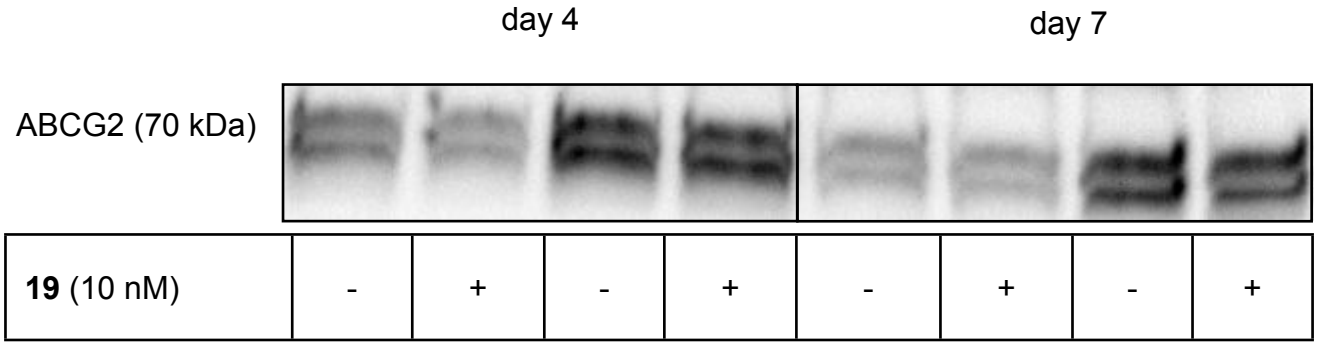

4 (0.5 µM)	-	-	+	+	-	-	+	+

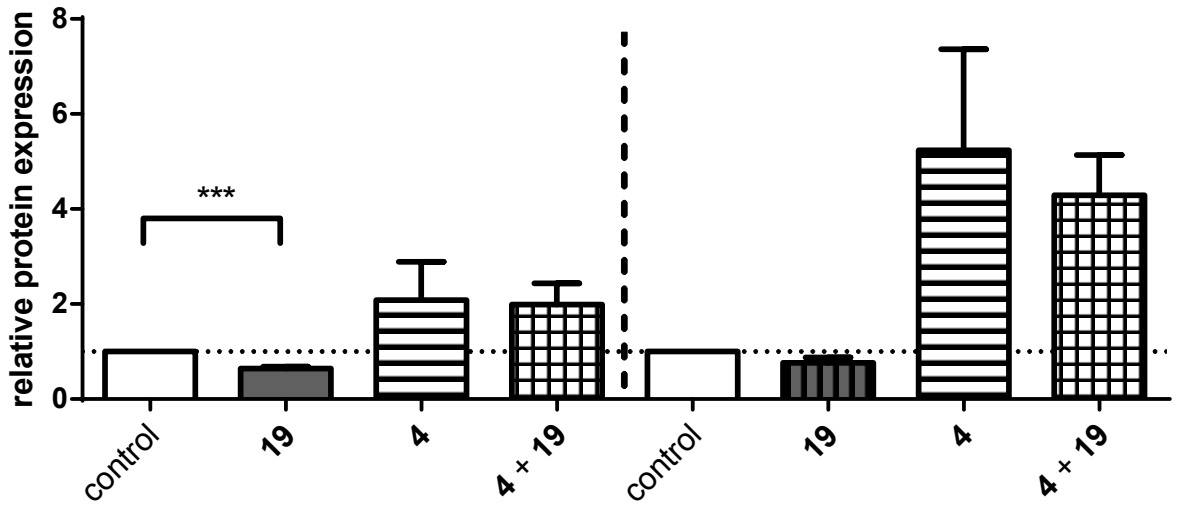

Figure 15: Western blot analysis of ABCG2 protein expression in MDCK II BCRP cells exposed to compound **19** (10 nM) and/or compound **4** (0.5 µM) for 4 (left) and 7 days (right), respectively. Bands were normalized by stain-free total protein normalization and related to each untreated control sample. Shown is mean ± SEM of at least three independent experiments. Significance was calculated applying one-sample *t*-test and is given as *: $p \leq 0.05$, **: $p \leq 0.01$, ***: $p \leq 0.001$, **** $p \leq 0.0001$.

Conclusion

The aim of this work was the exploration of the pyrimidine class as ABCG2-selective as well as broad-spectrum ABCB1/ABCC1/ABCG2 inhibitors based on our previous reports.[55,57] Only 7 of these derivatives have been reported previously and only one was evaluated for its capability to reverse ABCG2-mediated MDR (compound **10**),[57] and none for its broad-spectrum like reversal of ABCB1-, ABCC1-, and ABCG2-

mediated MDR. Within this work 23 further derivatives were generated. We found 7 (**19**, **21**-**22**, **29**-**31**, **33**) highly potent ABCG2 inhibitors which possessed IC_{50} values of ≤ 150 nM in either Hoechst 33342 and/or pheophorbide A assays, therefore significantly lower than the standard ABCG2 inhibitor **41**. Six of these compounds (**19**, **22**, **29**-**31**, **33**) exerted their inhibitory power in the high double-digit nanomolar concentration range, which makes them some of the most potent ABCG2 inhibitors known until today.[54,55,56,57,59,60,61] The most potent representatives (**19**, **22**, **29**-**31**) were proven to reverse ABCG2-mediated MDR in the low double-digit nanomolar concentration range, which is exceptional in literature.[55,56,57,59,60,61,89] Strikingly, the nontoxic and ABCG2-selective pyrimidine **19** had a half-maximal reversal concentration of only 11 nM, which makes it one of the 18 most potent ABCG2-mediated MDR reversers known until today.[56,89] Considering only data from the most commonly used 72h MTT-based MDR reversal assay in the literature, it represents the most potent reverser of ABCG2-mediated MDR. Further analysis of this compound showed that it not only concentration-dependently enhanced the cytotoxic effect of compound **4** in ABCG2-overexpressing cells, but also time-dependently increased compound **4** toxicity compared to compound **4** alone, doubling compound **4** toxicity in a time period of 7 days. A statistically significant difference was seen after five days, which correlates with a common topotecan treatment used in antineoplastic therapy (5-day-course).[98] While ~50 nM of compound **19** were sufficient to achieve half-maximal cell death at ~60% of the time in comparison to compound **4** treatment alone (t_{min}), only ~17.25 nM of compound **19** were necessary to half-maximally accelerate

half-maximal cell death in ABCG2-overexpressing cells when exposed to compound **4** ($C_{½tmax}$). There has never been a more detailed analysis of efficacy of a compound before, and these new measures could find implementation in future MDR reversal analysis.

Further analysis of the binding behavior of compound **19** showed that it bound to the Hoechst 33342 binding site of ABCG2 leading to competitive inhibition. Molecular docking studies based on cryo-EM structures of human ABCG2[99,100] with compound **19** revealed its strong and deep interaction with the S2 binding site of ABCG2 and supports our hypothesis regarding binding of quinazoline-based ABCG2 inhibitors as previously reported.[58]

Western blot analysis revealed that compound **19** did not lead to ABCG2 upregulation within four and seven days but rather led to a slight ABCG2 downregulation in these periods of time. This is important as induction of ABC transporters might lead to failure of chemotherapy in the first place.[19,20,21,22,23,24,25,30,31]

Taken together, its exceptional high inhibitory power against ABCG2, selectivity over ABCB1 and ABCC1, and extraordinary concentration- and time-dependent mediation of cell death in combination with a cytotoxic agent as well as its very low intrinsic toxicity and inability to induce ABCG2 makes compound **21** a promising candidate for further in vivo investigations.

As previous studies on selective ABC transporter inhibitors revealed frequently broad-spectrum ABC transporter modulators,[54,55,61,62,63,64,65,66] we further investigated the 23 pyrimidine derivatives for their mutli-target inhibition ability. Ten multi-target

ABCB1/ABCC1/ABCG2 inhibitors were discovered, which are up to now only presented by ~120 compounds in the literature. The potencies of five of these ranged within the 50 most potent compounds as known in literature.[38,49,54,55,61,62,63,64,65,66,74,75,76,77,78,79,80,81,82,83,84] Furthermore, compound **37** proved to reverse ABCB1-, ABCC1-, as well as ABCG2-mediated MDR in single-digit micromolar (ABCB1 and ABCC1) and double-digit nanomolar (ABCG2) concentration range. Only ~75 compounds have been reported with this ability before,[47,48,50,50,52,65,66,85,86,87,88,89] and hit compound **37** belongs to only 3 known compounds in the literature which have been proven to inhibit ABCB1, ABCC1, and ABCG2 as well as reversing ABCB1-, ABCC1-, ABCG2-mediated MDR.[65,66]

Cell viability assays indicated that the tested pyrimidines were rather nontoxic and furthermore not substrates of ABCG2. This hypothesis could be confirmed with confocal laser scanning microscopy using fluorescent pyrimidine **38**.

In essence, applying a highly interdisciplinary approach of chemical synthesis, living-cell based fluorescence- and absorbance accumulation assays, computational methods as well as protein quantification experiments, we continued the long-lasting development of ABCG2 inhibitors based on TKIs containing a quinazoline scaffold downsizing it until the basic scaffold was reached, which was superior in sensitizing ABCG2-overexpressing cells. These efforts revealed two exceptional and superior representatives, the ABCG2-selective compound **19** as well as the multi-target ABCB1/ABCC1/ABCG2 inhibitor and MDR reverser, compound **37.**

Experimental Section

Chemistry. *Materials.* Chemicals were purchased from Acros Organics (Geel, Belgium), Alfa Aesar (Karlsruhe, Germany), Sigma Aldrich (Steinheim, Germany), and Merck (Darmstadt, Germany). Microwave reactions were performed in 10 or 30 mL vials with a CEM Discover SP (CEM GmbH, Kamp-Lintfort, Germany). The reaction progress was monitored by thin layer chromatography (TLC) using an aluminum plate coated with silica gel 60 F_{254} (Merck Millipore, Billerica, MA, USA). Dichloromethane/methanol and ethyl acetate/petroleum ether (40-60 °C) were used as eluent. The identity of the compounds was confirmed by ^{1}H and ^{13}C NMR applying a Bruker Advance 500 MHz (500/126 MHz) or Bruker Advance 600 MHz (600/151 MHz). The chemical shifts (δ) were expressed in ppm. For the assignment of some ^{13}C signals, attached proton test (APT) was used. Multiplicity of the signals is indicated as singlet (s), doublet (d), doublet of doublets (dd), triplet of doublets (td), triplet (t), doublet of triplets (dt), quartet (q) and multiplet (m). The purity and molecular mass of compounds was confirmed by LC-MS analysis (Applied Biosystems API 2000 LC-MS/MS, HPLC Agilent 1100) using a photodiode array detector and a Nucleodur column 100-5 C18 (Macherey-Nagel, Düren, Germany) followed by ESI mass spectrometry using an API 2000 triple quadrupole mass spectrometer and Sciex Analyst software version 1.5.1. The purity of all compounds investigated in biological testing was determined as $\geq$95%.

Preparation of 6-methyl-2-phenylpyrimidin-4-ol (**13**). Sodium (0.304 g, 13.2 mmol) was dissolved in 50 ml ethanol to afford sodium ethoxide solution. Subsequently, benzamidine (1.31 g, 10.88 mmol), dissolved in 10 ml ethanol, and ethyl acetoacetate

(1.428 g, 10.97 mmol) were added to the sodium ethoxide solution, respectively. The resulting mixture was heated to reflux overnight and cooled down to room temperature. After solvent had been removed under reduced pressure, 20 ml water was added to the solid and the mixture was acidified with concentrated HCl to pH 5-6. The formed precipitate was vacuum filtered and washed with water three times. Finally, the obtained crude residue was recrystallized from DMF/H_2O to give 6-methyl-2-phenylpyrimidin-4-ol as white solid (1.22 g; 60%). ^{1}H NMR (500 MHz, DMSO-d_6) δ: 12.49 (s, 1H), 8.13 – 8.09 (m, 2H), 7.58 – 7.55 (m, 1H), 7.53 – 7.49 (m, 2H), 6.20 (s, 1H), 2.28 (d, J = 0.9 Hz, 3H). ^{13}C NMR (126 MHz, DMSO) δ: 164.56, 163.59, 156.92, 132.71, 131.42, 128.51, 127.68, 109.87, 23.45.

*Preparation of 4-chloro-6-methyl-2-phenylpyrimidine (***14***)*. The comound was synthesized from **13** (1.035 g, 5.07 mmol) and $POCl_3$ (20 ml). The solution was refluxed until the reaction was complete. Excess $POCl_3$ was removed under reduced pressure. The oily residue was transfered onto crushed ice portion by portion while keeping the temperature of solution below 10°C. The product was extracted three times with ethyl acetate. The organic layer was washed with saturated $NaHCO_3$, saturated NaCl solution and dried over magnesium sulfate. After filtration, ethyl acetate was removed under reduced pressure. Final purification was performed by column chromatography with ethyl acetate/petroleum ether (40-60 °C) = 1:8 as eluent to yield white crystals (0.782 g; 75%). ^{1}H NMR (600 MHz, Chloroform-*d*) δ: 8.47 – 8.44 (m, 2H), 7.52 – 7.47 (m, 3H), 7.11 (s, 1H), 2.60 (s, 3H). ^{13}C NMR (126 MHz, DMSO) δ: (151 MHz, $CDCl_3$) δ 169.02, 165.05, 161.69, 136.27, 131.53, 128.75, 128.73, 118.59, 24.14.

*General procedure for the preparation of 4-anilino-6-methyl-2-phenylpyrimidine derivatives (***18**-**40***)*. A mixture of one equivalent **14** and one equivalent of substituted aniline in 3 ml isopropanol were heated to 110 °C in microwave for 15-30 min. If reaction did not initiate, 0.1 equivalent of conc. HCl was added as catalyst. The precipitate was filtered off and washed with saturated sodium bicarbonate solution three times followed by distilled water three times. Further purification was performed by recrystallization or column chromatography.

*4-((6-methyl-2-phenylpyrimidin-4-yl)amino)phthalonitrile (***18***).* The title compound was synthesized from **14** (145 mg, 0.71 mmol) and 3,4-dicyanoaniline (101 mg, 0.70 mmol) as described in the general procedure above. Further purification was performed by recrystallization from ethanol/H_2O, white solid (13.6 mg, 6.2%). ^{1}H NMR (500 MHz, DMSO-d_6) δ: 10.35 (s, 1H), 8.54 (d, *J* = 2.2 Hz, 1H), 8.33 – 8.30 (m, 2H), 8.15 (dd, *J* = 2.2, 8.8 Hz, 1H), 8.05 (d, *J* = 8.7 Hz, 1H), 7.53 – 7.50 (m, 3H), 6.69 (s, 1H), 2.45 (s, 3H). ^{13}C NMR (126 MHz, DMSO) δ: 166.44, 162.47, 159.77, 144.84, 137.38, 134.88, 130.68, 128.51, 127.64, 122.81, 122.53, 116.41, 116.05, 115.29, 105.28, 105.11, 23.86. LC-MS (m/z) Calcd. for $C_{19}H_{13}N_5$ $[M+1]^+$: 312.12, Found: 312.2, Purity: 92%.

*2-methyl-4-((6-methyl-2-phenylpyrimidin-4-yl)amino)benzonitrile (***19***).* The title compound was synthesized from **14** (149 mg, 0.73 mmol) and 4-cyano-3-methylaniline (95 mg, 0.72 mmol) as described in the general procedure above. Further purification was performed by recrystallization from ethanol, white solid (103.9 mg, 48%). ^{1}H NMR (500 MHz, DMSO-d_6) δ: 9.94 (s, 1H), 8.38 – 8.33 (m, 2H), 7.92 (d, *J* = 1.7 Hz, 1H), 7.81 (dd, *J* = 2.2, 8.6 Hz, 1H), 7.73 (d, *J* = 8.5 Hz, 1H), 7.55 – 7.49 (m, 3H), 6.66 (s,

1H), 2.43 (s, 3H). ^{13}C NMR (126 MHz, DMSO) δ: 165.68, 162.46, 160.22, 144.37, 142.29, 137.65, 133.41, 130.46, 128.47, 127.64, 119.74, 118.50, 116.60, 104.60, 103.65, 23.83, 20.34. LC-MS (m/z) Calcd. for $C_{19}H_{16}N_4$ $[M+1]^+$: 301.14, Found: 301.1, Purity: 99%

*2-(4-((6-methyl-2-phenylpyrimidin-4-yl)amino)phenyl)acetonitrile (***20***).* The title compound was synthesized from **14** (105 mg, 0.51 mmol) and 2-(4-aminophenyl)acetonitrile (65 mg, 0.49 mmol) as described in the general procedure above. Further purification was performed by column chromatography, dichloromethane/methanol = 200:1 to 20:1. White solid (113.4 mg, 77%). ^{1}H NMR (500 MHz, DMSO-d_6) δ: 9.58 (s, 1H), 8.37 – 8.33 (m, 2H), 7.81 – 7.76 (m, 2H), 7.53 – 7.48 (m, 3H), 7.36 (d, *J* = 8.6 Hz, 2H), 6.58 (d, *J* = 0.8 Hz, 1H), 3.99 (s, 2H), 2.39 (s, 3H). ^{13}C NMR (126 MHz, DMSO) δ: 164.87, 162.40, 160.59, 139.46, 137.89, 130.24, 128.51, 128.35, 127.61, 124.50, 120.02, 119.37, 103.46, 23.77, 21.77. LC-MS (m/z) Calcd. for $C_{19}H_{16}N_4$ $[M+1]^+$: 301.14, Found: 301.0, Purity: 99%.

*6-methyl-N-(3-nitrophenyl)-2-phenylpyrimidin-4-amine (***21***).* The title compound was synthesized from **14** (71 mg, 0.35 mmol) and 3-nitroaniline (49 mg, 0.35 mmol) as described in the general procedure above. Further purification was performed by recrystallization from isopropanol/H_2O, yellow solid (22.5 mg, 21%). ^{1}H NMR (500 MHz, DMSO-d_6) δ: 10.06 (s, 1H), 9.24 (t, *J* = 2.2 Hz, 1H), 8.46 – 8.42 (m, 2H), 7.95 (ddd, *J* = 0.9, 2.2, 8.2 Hz, 1H), 7.86 (ddd, *J* = 0.9, 2.3, 8.1 Hz, 1H), 7.64 (t, *J* = 8.1 Hz, 1H), 7.56 – 7.48 (m, 3H), 6.64 (d, *J* = 0.8 Hz, 1H), 4.30 (d, *J* = 4.3 Hz, 0H), 2.44 (d, *J* = 0.6

Hz, 3H), ^{13}C NMR (126 MHz, DMSO) δ: 13C NMR (126 MHz, DMSO) δ 165.51, 162.35, 160.30, 148.09, 141.44, 137.60, 130.52, 129.97, 128.41, 127.69, 124.95, 116.05, 113.24, 104.30, 23.83. LC-MS (m/z) Calcd. for $C_{17}H_{14}N_4O_2$ $[M+1]^+$: 307.11, Found: 307.1, Purity: 99%.

*6-methyl-N-(4-nitrophenyl)-2-phenylpyrimidin-4-amine (***22***).* The title compound was synthesized from **14** (100 mg, 0.49 mmol) and 4-nitroaniline (68 mg, 0.49 mmol) as described in the general procedure above. Further purification was performed by recrystallization from isopropanol/H_2O, yellow solid (18.7 mg, 13%). ^{1}H NMR (500 MHz, DMSO-d_6) δ: 10.25 (s, 1H), 8.41 – 8.37 (m, 2H), 8.32 – 8.28 (m, 2H), 8.09 – 8.05 (m, 2H), 7.57 – 7.51 (m, 3H), 6.72 (d, *J* = 0.7 Hz, 1H), 2.46 (d, *J* = 0.6 Hz, 3H). ^{13}C NMR (126 MHz, DMSO) δ: 166.03, 162.55, 160.03, 146.72, 140.70, 137.47, 130.55, 128.52, 127.78, 125.15, 118.39, 105.00, 23.86. LC-MS (m/z) Calcd. for $C_{17}H_{14}N_4O_2$ $[M+1]^+$: 307.11, Found: 307.2, Purity: 99%.

*3-((6-methyl-2-phenylpyrimidin-4-yl)amino)phenol (***23***).* The title compound was synthesized from **14** (210 mg, 1.03 mmol) and 3-bromoaniline (113 mg, 1.04 mmol) as described in the general procedure above. Further purification was performed by recrystallization from chloroform/n-hexane, white solid (122.9 mg, 43%). ^{1}H NMR (500 MHz, DMSO-d_6) δ: 9.36 (s, 2H), 8.39 – 8.34 (m, 2H), 7.52 – 7.46 (m, 3H), 7.26 (dd, *J* = 1.6, 2.7 Hz, 1H), 7.17 – 7.11 (m, 2H), 6.56 (d, *J* = 0.7 Hz, 1H), 6.45 (dt, *J* = 2.3, 6.6 Hz, 1H), 2.38 (d, *J* = 0.6 Hz, 3H). ^{13}C NMR (126 MHz, DMSO) δ: 164.64, 162.45, 160.74, 157.74, 141.03, 137.99, 130.16, 129.36, 128.28, 127.68, 110.55, 109.47,

106.88, 103.32, 23.79. LC-MS (m/z) Calcd. for $C_{17}H_{15}N_3O$ $[M+1]^+$: 278.12, Found: 278.1, Purity: 99%.

*(3-((6-methyl-2-phenylpyrimidin-4-yl)amino)phenyl)methanol (***24***).* The title compound was synthesized from **14** (103 mg, 0.50 mmol) and (4-aminophenyl)methanol (62 mg, 0.50 mmol) as described in the general procedure above. Further purification was performed by column chromatography, dichloromethane/methanol = 200:1 to 20:1. White solid (83.1 mg, 57%). ^{1}H NMR (500 MHz, DMSO-d_6) δ: 9.81 (s, 1H), 8.39 – 8.33 (m, 2H), 7.82 (s, 1H), 7.61 (dt, *J* = 1.6, 8.0 Hz, 1H), 7.55 – 7.49 (m, 3H), 7.33 (t, *J* = 7.8 Hz, 1H), 7.01 (d, *J* = 7.5 Hz, 1H), 6.63 (s, 1H), 5.21 (s, 1H), 4.55 (s, 2H), 2.42 (s, 3H). ^{13}C NMR (126 MHz, DMSO) δ: 163.23, 161.78, 160.76, 143.34, 139.43, 136.70, 130.70, 128.42, 127.86, 120.65, 118.33, 118.18, 103.38, 62.84, 22.98. LC-MS (m/z) Calcd. for $C_{18}H_{17}N_3O$ $[M+1]^+$: 292.14, Found: 292.1, Purity: 98%.

*N-(3-methoxyphenyl)-6-methyl-2-phenylpyrimidin-4-amine (***25***).* The title compound was synthesized from **14** (182 mg, 0.89 mmol) and 3-methoxyaniline (186 mg, 1.51 mmol) as described in the general procedure above. Further purification was performed by recrystallization from isopropanol, white solid (23.6 mg, 9.1%). ^{1}H NMR (500 MHz, DMSO-d_6) δ: 9.51 (s, 1H), 8.38 – 8.34 (m, 2H), 7.59 (t, *J* = 2.1 Hz, 1H), 7.53 – 7.47 (m, 3H), 7.29 – 7.22 (m, 2H), 6.61 (ddd, *J* = 1.7, 2.5, 7.6 Hz, 1H), 6.58 (d, *J* = 0.8 Hz, 1H), 3.80 (s, 3H), 2.39 (d, *J* = 0.6 Hz, 3H). ^{13}C NMR (126 MHz, DMSO) δ: 164.81, 162.41, 160.67, 159.62, 141.31, 138.00, 130.24, 129.46, 128.31, 127.55, 111.83, 107.86, 105.12, 103.59, 54.94, 23.79. LC-MS (m/z) Calcd. for $C_{18}H_{17}N_3O$ $[M+1]^+$: 292.14, Found: 292.0, Purity: 99%

*N-(3-fluorophenyl)-6-methyl-2-phenylpyrimidin-4-amine (**26**).* The title compound was synthesized from **14** (193 mg, 0.94 mmol) and 3-fluoroaniline (108 mg, 0.97 mmol) as described in the general procedure above. Further purification was performed by recrystallization from n-hexane, white solid (134.1 mg, 51%). ^{1}H NMR (500 MHz, DMSO-d_6) δ: 9.73 (s, 1H), 8.37 – 8.32 (m, 2H), 7.86 (dt, *J* = 2.3, 12.2 Hz, 1H), 7.55 – 7.48 (m, 3H), 7.46 (ddd, *J* = 1.0, 2.0, 8.3 Hz, 1H), 7.39 (td, *J* = 6.9, 8.2 Hz, 1H), 6.84 (tdd, *J* = 0.9, 2.6, 8.5 Hz, 1H), 6.61 (d, *J* = 0.8 Hz, 1H), 2.41 (d, *J* = 0.6 Hz, 3H). ^{13}C NMR (126 MHz, DMSO) δ: 165.17, 162.44, 161.76 (d, *J* = 240.6 Hz), 160.47, 142.00, 137.86, 130.35, 130.26 (d, *J* = 9.6 Hz), 128.41, 127.54, 115.12, 108.19 (d, *J* = 21.5 Hz), 106.05 (d, *J* = 26.2 Hz),103.91, 23.80. LC-MS (m/z) Calcd. for $C_{17}H_{14}FN_3$ $[M+1]^+$: 280.12, Found: 280.1, Purity: 98%.

*N-(3-chlorophenyl)-6-methyl-2-phenylpyrimidin-4-amine (**27**).* The title compound was synthesized from **14** (168 mg, 0.82 mmol) and 3-chloroaniline (102 mg, 0.80 mmol) as described in the general procedure above. Further purification was performed by recrystallization from n-hexane, white solid (148.7 mg, 63%). ^{1}H NMR (500 MHz, DMSO-d_6) δ: 9.72 (s, 1H), 8.39 – 8.31 (m, 2H), 8.11 (t, *J* = 2.1 Hz, 1H), 7.62 (ddd, *J* = 0.9, 2.1, 8.3 Hz, 1H), 7.56 – 7.46 (m, 3H), 7.39 (t, *J* = 8.1 Hz, 1H), 7.07 (ddd, *J* = 0.9, 2.2, 8.0 Hz, 1H), 6.60 (d, *J* = 0.8 Hz, 1H), 2.41 (d, *J* = 0.6 Hz, 3H). ^{13}C NMR (126 MHz, DMSO) δ: 165.22, 162.37, 160.40, 141.64, 137.82, 133.03, 130.38, 130.34, 128.39, 127.54, 121.42, 118.90, 117.69, 103.93, 23.80. LC-MS (m/z) Calcd. for $C_{17}H_{14}ClN_3$ $[M+1]^+$: 296.09, Found: 296.1, Purity: 99%.

*N-(3-bromophenyl)-6-methyl-2-phenylpyrimidin-4-amine (***28***).* The title compound was synthesized from **14** (123 mg, 0.60 mmol) and 3-bromoaniline (102 mg, 0.60 mmol) as described in the general procedure above. Further purification was performed by recrystallization from n-hexane, white solid (44.7 mg, 22%). ^{1}H NMR (500 MHz, DMSO-d_6) δ: 9.71 (s, 1H), 8.38 – 8.32 (m, 2H), 8.29 (t, *J* = 2.0 Hz, 1H), 7.65 (ddd, *J* = 0.9, 2.1, 8.2 Hz, 1H), 7.56 – 7.47 (m, 3H), 7.33 (t, *J* = 8.1 Hz, 1H), 7.20 (ddd, *J* = 0.9, 1.9, 7.9 Hz, 1H), 6.59 (d, *J* = 0.7 Hz, 1H), 2.41 (d, *J* = 0.7 Hz, 3H). ^{13}C NMR (126 MHz, DMSO) δ: 165.22, 162.34, 160.36, 141.78, 137.80, 130.63, 130.39, 128.38, 127.55, 124.28, 121.83, 121.53, 118.04, 103.93, 23.81. LC-MS (m/z) Calcd. for $C_{17}H_{14}BrN_3$ $[M+1]^+$: 340.04, Found: 340.1, Purity: 99%.

*2-fluoro-5-((6-methyl-2-phenylpyrimidin-4-yl)amino)benzonitrile (***29***).* The title compound was synthesized from **14** (101 mg, 0.49 mmol) and 3-cyano-4-fluoroaniline (66 mg, 0.48 mmol) as described in the general procedure above. Further purification was performed by column chromatography, ethyl acetate/petroleum ether (40-60 °C) = 1:8 to 1:1. White solid (117.6 mg, 80%). ^{1}H NMR (500 MHz, DMSO-d_6) δ: 9.84 (s, 1H), 8.34 – 8.29 (m, 3H), 8.02 (ddd, *J* = 2.8, 4.8, 9.2 Hz, 1H), 7.56 – 7.47 (m, 4H), 6.59 (s, 1H), 2.41 (s, 3H). ^{13}C NMR (126 MHz, DMSO) δ: 165.45, 162.35, 160.21, 157.34 (d, *J* = 250.7 Hz), 137.71, 137.31 (d, *J* = 2.4 Hz), 130.42, 128.38, 127.56, 126.67 (d, *J* = 7.8 Hz), 123.15, 116.98 (d, *J* = 20.6 Hz), 114.13, 103.77, 99.77 (d, *J* = 16.1 Hz), 23.80. LC-MS (m/z) Calcd. for $C_{18}H_{13}FN_4$ $[M+1]^+$: 305.11, Found: 305.1, Purity: 98%.

*2-bromo-4-((6-methyl-2-phenylpyrimidin-4-yl)amino)benzonitrile (***30***).* The title compound was synthesized from **14** (102 mg, 0.50 mmol) and 3-bromo-4-cyanoaniline

(97 mg, 0.49 mmol) as described in the general procedure above. Further purification was performed by column chromatography, ethyl acetate/petroleum ether (40-60 °C) = 1:8 to 1:1. White solid (93.4 mg, 52%). ^{1}H NMR (500 MHz, DMSO-d_6) δ: 10.94 (s, 1H), 8.57 (s, 1H), 8.32 – 8.29 (m, 2H), 7.93 – 7.87 (m, 2H), 7.63 – 7.55 (m, 3H), 6.85 (s, 1H), 2.51 (s, 3H). ^{13}C NMR (126 MHz, DMSO) δ: 163.28, 161.39, 160.27, 144.78, 135.29, 131.57, 128.71, 128.05, 124.86, 122.84, 118.61, 117.65, 106.71, 105.29, 22.41. LC-MS (m/z) Calcd. for $C_{18}H_{13}BrN_4$ $[M+1]^+$: 365.03, Found: 365.0, Purity: 97%.

*4-((6-methyl-2-phenylpyrimidin-4-yl)amino)-2-(trifluoromethyl)benzonitrile (***31***).* The title compound was synthesized from **14** (153 mg, 0.75 mmol) and 4-cyano-3-trifluoroaniline (139 mg, 0.74 mmol) as described in the general procedure above. Further purification was performed by recrystallization from ethanol, white solid (59.0 mg, 22%). ^{1}H NMR (500 MHz, DMSO-d_6) δ: 10.41 (s, 1H), 8.84 (s, 1H), 8.37 – 8.31 (m, 2H), 8.09 (d, J = 8.7 Hz, 1H), 8.02 (d, J = 8.8 Hz, 1H), 7.57 – 7.47 (m, 3H), 6.70 (s, 1H), 2.46 (s, 3H). ^{13}C NMR (126 MHz, DMSO) δ: 166.32, 162.41, 159.90, 144.95, 137.36, 136.19, 131.70 (q, J = 31.6 Hz), 130.69, 128.46, 127.57, 122.26 (q, J = 273.2 Hz), 121.41, 116.16, 116.10, 105.15, 99.16, 23.86. LC-MS (m/z) Calcd. for $C_{19}H_{13}F_3N_4$ $[M+1]^+$: 355.11, Found: 355.1, Purity: 99%.

*N-(4-fluoro-3-nitrophenyl)-6-methyl-2-phenylpyrimidin-4-amine (***32***).* The title compound was synthesized from **14** (98 mg, 0.48 mmol) and 4-fluoro-3-nitroaniline (68 mg, 0.44 mmol) as described in the general procedure above. Further purification was performed by column chromatography, dichloromethane/methanol = 200:1 to 20:1. Yellow solid (96.5 mg, 68%). ^{1}H NMR (500 MHz, DMSO-d_6) δ: 9.99 (s, 1H), 9.11 (dd,

J = 2.8, 6.9 Hz, 1H), 8.43 – 8.38 (m, 2H), 7.90 (ddd, *J* = 2.8, 3.8, 9.1 Hz, 1H), 7.58 (dd, *J* = 9.0, 11.2 Hz, 1H), 7.54 – 7.48 (m, 3H), 6.60 (d, *J* = 0.8 Hz, 1H), 2.43 (s, 3H). ^{13}C NMR (126 MHz, DMSO) δ: 165.48, 162.31, 160.12, 149.49 (d, *J* = 257.1 Hz), 137.56, 137.04 (d, *J* = 3.2 Hz), 136.22 (d, *J* = 7.8 Hz), 130.51, 128.38, 127.68, 126.38 (d, *J* = 7.9 Hz), 118.71 (d, *J* = 22.1 Hz), 115.45 (d, *J* = 3.3 Hz), 104.06, 23.81. LC-MS (m/z) Calcd. for $C_{17}H_{13}FN_4O_2$ $[M+1]^+$: 325.10, Found: 324.9, Purity: 99%.

*N-(3-chloro-4-nitrophenyl)-6-methyl-2-phenylpyrimidin-4-amine (***33***).* The title compound was synthesized from **14** (114 mg, 0.56 mmol) and 3-chloro-4-nitroaniline (93 mg, 0.54 mmol) as described in the general procedure above. Further purification was performed by column chromatography, dichloromethane/methanol = 200:1 to 20:1. Pale yellow solid (75.0 mg, 41%). ^{1}H NMR (500 MHz, DMSO-d_6) δ: 11.14 (s, 1H), 8.39 (d, *J* = 2.3 Hz, 1H), 8.36 – 8.28 (m, 2H), 8.22 (d, *J* = 9.0 Hz, 1H), 7.94 (dd, *J* = 2.3, 9.0 Hz, 1H), 7.64 – 7.55 (m, 3H), 6.90 (s, 1H), 2.53 (s, 3H). ^{13}C NMR (126 MHz, DMSO) δ: 163.29, 161.33, 160.27, 144.61, 140.48, 135.06, 131.63, 128.73, 128.12, 127.72, 126.96, 121.13, 118.25, 105.35, 22.24. LC-MS (m/z) Calcd. for $C_{17}H_{13}ClN_4O_2$ $[M+1]^+$: 341.07, Found:341.2, Purity: 98%.

*N-(4-bromo-3-methoxyphenyl)-6-methyl-2-phenylpyrimidin-4-amine (***34***).* The title compound was synthesized from **14** (148 mg, 0.72 mmol) and 4-bromo-3-methoxyaniline (146 mg, 0.72 mmol) as described in the general procedure above. Further purification was performed by recrystallization from isopropanol/H_2O, white solid (34.4 mg, 13%). ^{1}H NMR (500 MHz, DMSO-d_6) δ: 9.67 (s, 1H), 8.39 – 8.34 (m, 2H), 7.87 (d, *J* = 2.4 Hz, 1H), 7.53 – 7.48 (m, 4H), 7.18 (dd, *J* = 2.4, 8.6 Hz, 1H), 6.60

(d, *J* = 0.8 Hz, 1H), 2.41 (d, *J* = 0.6 Hz, 3H). ^{13}C NMR (126 MHz, DMSO) δ: 165.21, 162.58, 160.62, 155.49, 141.23, 138.05, 132.73, 130.48, 128.50, 127.75, 112.90, 104.26, 104.08, 102.49, 56.06, 23.95. LC-MS (m/z) Calcd. for $C_{18}H_{16}BrN_3O$ $[M+1]^+$: 370.05, Found: 370.0, Purity: 99%.

*N-(3-fluoro-4-methoxyphenyl)-6-methyl-2-phenylpyrimidin-4-amine (***35***).* The title compound was synthesized from **14** (91 mg, 0.45 mmol) and 3-fluoro-4-methoxyaniline (60 mg, 0.42 mmol) as described in the general procedure above. Further purification was performed by column chromatography, ethyl acetate/petroleum ether (40-60 °C) = 1:8 to 1:1. White solid (84.0 mg, 64%). ^{1}H NMR (500 MHz, DMSO-d_6) δ: 9.49 (s, 1H), 8.35 – 8.30 (m, 2H), 7.76 (dd, *J* = 2.6, 13.9 Hz, 1H), 7.53 – 7.47 (m, 3H), 7.41 (ddd, *J* = 1.4, 2.6, 8.9 Hz, 1H), 7.19 (dd, *J* = 8.9, 9.8 Hz, 1H), 6.52 (d, *J* = 0.7 Hz, 1H), 3.84 (s, 3H), 2.38 (d, *J* = 0.6 Hz, 3H). ^{13}C NMR (126 MHz, DMSO) δ: 164.77, 162.40, 160.56, 151.04 (d, *J* = 241.9 Hz), 142.23 (d, *J* = 10.6 Hz), 137.97, 133.56 (d, *J* = 9.6 Hz), 130.24, 128.34, 127.52, 115.69, 114.37 (d, *J* = 3.0 Hz), 108.33 (d, *J* = 22.7 Hz), 103.16, 56.28, 23.77. LC-MS (m/z) Calcd. for $C_{18}H_{16}FN_3O$ $[M+1]^+$: 310.13, Found: 310.1, Purity: 100%.

*N-(4-methoxy-3-(trifluoromethyl)phenyl)-6-methyl-2-phenylpyrimidin-4-amine (***36***).* The title compound was synthesized from **14** (53 mg, 0.26 mmol) and 3-trifluoro-4-methoxyaniline (49 mg, 0.26 mmol) as described in the general procedure above. Further purification was performed by column chromatography, ethyl acetate/petroleum ether (40-60 °C) = 1:8 to 1:1. Brown solid (73.8 mg, 81%). ^{1}H NMR (500 MHz, DMSO-d_6) δ: 11.13 (s, 1H), 8.29 – 8.22 (m, 3H), 7.91 (d, *J* = 8.8 Hz, 1H),

7.67 (t, *J* = 7.4 Hz, 1H), 7.61 (t, *J* = 7.6 Hz, 2H), 7.37 (d, *J* = 9.0 Hz, 1H), 6.81 (s, 1H), 3.91 (s, 3H), 2.53 (s, 3H). ^{13}C NMR (126 MHz, DMSO) δ: 160.64, 160.60, 159.88, 153.61, 132.52, 130.88, 128.80, 128.42, 126.71, 123.50 (q, *J* = 272.5 Hz), 119.89, 116.78 (q, *J* = 27.5, 28.3 Hz), 113.69, 104.01, 56.39, 20.31. LC-MS (m/z) Calcd. for $C_{19}H_{16}F_3N_3O$ $[M+1]^+$: 360.12, Found: 360.0, Purity: 99%.

N-(6-methyl-2-phenylpyrimidin-4-yl)quinolin-6-amine (**37**). The title compound was synthesized from **14** (55 mg, 0.27 mmol) and quinolin-6-amine (46 mg, 0.32 mmol) as described in the general procedure above. Further purification was performed by recrystallization from ethyl acetate/n-hexane, yellow solid (13.5 mg, 16%). ^{1}H NMR (500 MHz, DMSO-d_6) δ: 9.88 (s, 1H), 8.76 (dd, *J* = 1.7, 4.2 Hz, 1H), 8.56 (d, *J* = 2.4 Hz, 1H), 8.43 – 8.39 (m, 2H), 8.31 – 8.28 (m, 1H), 8.03 – 7.94 (m, 2H), 7.57 – 7.47 (m, 4H), 6.69 (d, *J* = 0.8 Hz, 1H), 2.43 (s, 3H). ^{13}C NMR (126 MHz, DMSO) δ: 165.15, 162.54, 160.62, 148.44, 144.24, 138.10, 137.89, 135.14, 130.32, 129.41, 128.52, 128.47, 127.68, 124.18, 121.74, 114.56, 103.89,23.85. LC-MS (m/z) Calcd. for $C_{20}H_{16}N_4$ $[M+1]^+$: 313.14, Found: 313.2, Purity: 99%.

*N-(6-methyl-2-phenylpyrimidin-4-yl)quinoxalin-6-amine (***38***).* The title compound was synthesized from **14** (120 mg, 0.58 mmol) and quinoxalin-6-amine (85 mg, 0.58 mmol) as described in the general procedure above. Further purification was performed by recrystallization from ethanol/H_2O, brown solid (38.2 mg, 21%). ^{1}H NMR (500 MHz, DMSO-d_6) δ: 10.11 (s, 1H), 8.88 (dd, *J* = 2.1, 14.2 Hz, 2H), 8.78 (d, *J* = 1.8 Hz, 1H), 8.45 – 8.42 (m, 2H), 8.08 – 8.02 (m, 2H), 7.57 – 7.53 (m, 3H), 6.74 (d, *J* = 0.8 Hz, 1H), 2.46 (d, *J* = 0.6 Hz, 3H). ^{13}C NMR (126 MHz, DMSO) δ: 165.46, 162.59, 160.48, 145.84,

143.47, 143.20, 141.50, 138.63, 137.83, 130.51, 129.43, 128.50, 127.66, 124.48, 114.63, 104.60,23.88. LC-MS (m/z) Calcd. for $C_{19}H_{15}N_5$ $[M+1]^+$: 314.13, Found: 314.0, Purity: 99%.

*N-(2,3-dihydrobenzo[b][1,4]dioxin-6-yl)-6-methyl-2-phenylpyrimidin-4-amine (***39***).* The title compound was synthesized from **14** (102 mg, 0.50 mmol) and 2,3-dihydrobenzo[*b*][1,4]dioxin-6-amine (71 mg, 0.47 mmol) as described in the general procedure above. Further purification was performed by column chromatography, ethyl acetate/petroleum ether (40-60 °C) = 1:8 to 1:1. Beige solid (123.8 mg, 84%). ^{1}H NMR (500 MHz, DMSO-d_6) δ: 9.65 (s, 1H), 8.34 – 8.26 (m, 2H), 7.56 – 7.48 (m, 3H), 7.38 (s, 1H), 7.09 (dd, *J* = 2.5, 8.7 Hz, 1H), 6.87 (d, *J* = 8.7 Hz, 1H), 6.55 (s, 1H), 4.30 – 4.20 (m, 4H), 2.39 (s, 3H). ^{13}C NMR (126 MHz, DMSO) δ: 161.96, 160.92, 143.26, 139.41, 133.19, 130.84, 128.57, 127.89, 117.09, 113.90, 109.62, 103.05, 64.38, 64.09, 23.02. LC-MS (m/z) Calcd. for $C_{19}H_{17}N_3O_2$ $[M+1]^+$: 320.13, Found: 319.8, Purity: 99%.

*5-((6-methyl-2-phenylpyrimidin-4-yl)amino)isoindoline-1,3-dione (***40***).* The title compound was synthesized from **14** (100 mg, 0.49 mmol) and 5-aminoisoindoline-1,3-dione (75 mg, 0.47 mmol) as described in the general procedure above. Further purification was performed by column chromatography, dichloromethane/methanol = 200:1 to 20:1. Yellow solid (31.7 mg, 21%). ^{1}H NMR (500 MHz, DMSO-d_6) δ: 11.17 (s, 1H), 10.58 (s, 1H), 8.46 (d, *J* = 1.9 Hz, 1H), 8.35 (dd, *J* = 1.9, 7.8 Hz, 2H), 8.06 (dd, *J* = 1.9, 8.3 Hz, 1H), 7.83 (d, *J* = 8.2 Hz, 1H), 7.61 – 7.51 (m, 3H), 6.78 (s, 1H), 2.48 (s, 3H). ^{13}C NMR (126 MHz, DMSO) δ: 169.20, 169.02, 161.98, 160.51, 145.45, 136.42,

134.42, 131.30, 128.76, 128.08, 125.47, 124.22, 123.86, 113.21, 104.98, 23.09. LC-MS (m/z) Calcd. for $C_{19}H_{14}N_4O_2$ $[M+1]^+$: 331.11, Found: 331.1, Purity: 96%.

Biological Investigations

Materials. The reference compounds **41** ((3S,6S,12aS)-1,2,3,4,6,7,12,12a-octahydro-9-methoxy-6-(2-methylpropyl)-1,4-dioxopyrazino[1',2':1,6]pyrido[3,4-*b*]indole-3-propanoic acid 1,1-dimethylethylester) and cyclosporine A were purchased from Tocris Bioscience (Bristol, UK). The fluorescence dyes pheophorbide A and calcein AM were provided by Calbiochem [EMD Chemicals (San Diego, USA), supplied by Merck KgaA (Darmstadt, Germany)]. All other chemicals were purchased from Sigma-Aldrich (Taufkirchen, Germany), Carl Roth (Karlsruhe, Germany) or Merck KgaA (Darmstadt, Germany). The compounds and references were prepared as 10 mM stock solutions in DMSO and stored at -20 °C. Cell-based assays were carried out in Krebs-HEPES buffer (KHB) at pH of 7,4. KHB was prepared from 118.6 mM NaCl, 4.7 mM KCl, 1.2 mM KH_2PO_4, 4.2 mM $NaHCO_3$, 1.3 mM $CaCl_2$, 1.2 mM $MgSO_4$, 11.7 mM D-glucose monohydrate, and 10.0 mM HEPES (2-[4-(2-hydroxyethyl)piperazin-1-yl]ethanesulfonic acid) in doubly distilled water. The pH of the solution was adjusted to 7,4 at 37 °C with sodium hydroxide solution and then it was sterilized using a 0.2 μM membrane filter.

Cell Culture. The cell lines MDCK II, MDCK II BCRP and MDCK II MRP1 were received as a generous gift from Dr. A. Schinkel (The Netherlands Cancer Institute, Amsterdam,

The Netherlands). MDCK II BCRP cells were generated by transfection of the canine kidney epithelial cell line MDCK II with the human wild-type cDNA C-terminally linked to the cDNA of the green fluorescent protein (GFP).[101] These cells were cultured in Dulbecco's modified eagle medium (DMEM) supplemented with 10% fetal bovine serum (FCS), 50 µg/µL streptomycin, 50 U/mL penicillin G and 2 mM L-glutamine. Human ovarian carcinoma cell line A2780/ADR was purchased from European Collection of Animal Cell Culture (ECACC, no. 93112520) and cultured in RPMI-1640 medium supplemented with 10% FCS, 50 µg/µL streptomycin, 50 U/mL penicillin G and 2 mM L-glutamine. To preserve the doxorubicin resistance every 10 passages the cells were grown with 1 µM doxorubicin for one passage. The breast cancer cell lines MCF-7 and MCF-7/MX were a generous gift from Dr. Erasmus Schneider (Wadsworth Center, Albany, NY, US).[4] The cells were cultured in RPMI 1640 culture medium supplemented with 20% FCS, 50 U/mL penicillin G, and 2 mM L-glutamine. All the cells were stored under liquid nitrogen in a mixture of 90% pure cell culture medium and 10% DMSO. Cell culturing was performed in 5% CO_2-humidified atmosphere at 37 °C. Harvesting was conducted after a confluence of at least 90% was achieved for either sub-culturing or biological evaluation. The cells were detached with 0.05% trypsin and 0.02% EDTA, collected with medium and centrifuged in a 50 mL falcon (266 x *g*, 4 °C, 4 min). After removing the supernatant cells were re-suspended in fresh culture medium. If cells were used for cell-based assays they were afterwards washed with KHB three times in order to remove excess culture medium. The cell count was

determined by a CASY TT cell counter (Schärfe System GmbH, Reutlingen, Germany) equipped with a 150 µm capillary.

Hoechst 33342 Assay. To investigate the inhibitory effect of the compounds on ABCG2, a Hoechst 33342 assay was performed as described earlier.[58,102] Dilutions of the compounds were prepared in KHB with addition of a certain amounts of methanol in case of solubility problems, which resulted in a final methanol concentration of less than 5%. 20 µL of the prepared dilutions were placed into black 96 well plates (Greiner, Frickenhausen, Germany). Cells were harvested as described before and then seeded into prepared plates at a density of approximately 30,000 cells per well in a volume of 160 µL. Following the pre-incubation of 30 min at 37 °C and 5% CO_2, 20 µL of 10 µM Hoechst 33342 solution were added to each well, amounting to a final concentration of 1 µM Hoechst 33342. Fluorescence was measured in constant time intervals of 60 s for 120 min with an excitation wavelength of 355 nm and an emission wavelength of 460 nm using microplate readers (POLARstar and FLUOstar Optima by BMG Labtech, Offenburg, Germany). Average of fluorescence values in the steady state were calculated for each concentration and plotted against the logarithm of the compound concentration. Concentration-response curves were generated by nonlinear regression using the three- or four-parameter logistic equation. The statistically preferred model was chosen for calculating IC_{50} value (GraphPad Prism, version 6.0, San Diego, CA, USA).

Pheophorbide A Assay. Additionally, the inhibitory potency against ABCG2 was examined using the pheophorbide A assay as described earlier.[90] 20 µL of the compound dilutions were pipetted into 96-well U-shaped clear plates (Greiner, Frickenhausen, Germany) and the cell suspension was prepared. Approximately 45,000 cells were added to each well in a volume of 160 µL and the plate was kept for 15 min at 37 °C and 5% CO_2. Afterwards, 20 µL of 5 µM pheophorbide A solution were added yielding a final concentration of 0.5 µM. The plate was incubated for 2 h and then measured at an excitation wavelength of 488 nm and emission of 695/50 nm using Guava easyCyte™ HT flow cytometry. Expression of ABCG2 was examined by the fluorescence of GFP detected at the wavelength of 525/30 nm. Data analysis was performed as described for the Hoechst 33342 assay.

Calcein AM Assay. The calcein AM assay assay was performed to determine the selectivity of the compounds as already described earlier.[90,81] The compounds were tested for their inhibitory activity towards ABCB1 and ABCC1 using A2780/ADR and MDCK II MRP1 cells, respectively. 20 µL of the compound dilutions were put into a 96-well flat-bottom clear plate (Greiner, Frickenhausen, Germany). After the cells were harvested and washed as described earlier, the cells were seeded into the plate at a density of 30,000 cells per well. The addition of the cell suspension to the dilutions of the compounds resulted in a total amount of 180 µL which were thereafter incubated for 30 min at 37 °C and 5% CO_2. Afterwards, 20 µL of a 3.125 µM calcein AM solution were added to each well and immediately measured every 60 s for a period of 60 min. The measurement was carried out at the excitation wavelength of 485 nm and

emission of 520 nm using a microplate reader (POLARstar and FLUOstar Optima by BMG Labtech, Offenburg, Germany). The first linear increase of fluorescence was used for calculating slopes, which were then plotted against logarithmic concentrations of tested compounds. Data analysis was performed as described above.

MTT Cell Viability Assay. Intrinsic cytotoxicity of the compounds was determined by a MTT viability assay as described earlier.[90,81] Solutions of test compounds in culture medium were prepared in concentrations ranging from 3.2 to 1000 µM. After these dilution series were pipetted into 96 well tissue culture plates (Starlab GmbH, Hamburg, Germany) cells were harvested as described before. MDCK II BCRP and the parental cells were seeded at a density of approximately 2,000 cells per well in a volume of 180 µL culture medium and stored under 5% CO_2 and 37°C for 72 h. Culture medium and 10% (v/v) DMSO were used as negative and positive control, respectively, and determined 100% and 0% viability, respectively. After the incubation period of 72 h, 40 µL (5 mg/mL) of MTT reagent (3-(4,5-dimethylthiazol-2-yl)-2,5-diphenyltetrazolium bromide) were added to each well and incubated for 1 h. Afterwards, the supernatant was removed and the formed formazan was dissolved in 100 µL of DMSO. Absorbance was measured spectrophotometrically at 570 nm using an Ex Multiscan microplate photometer (Thermo Fischer Scientific, Waltham, MA, USA) with a background correction at 690 nm. The measured absorbance values were plotted against logarithmic concentrations and the half-maximal growth inhibition (GI_{50}) values were calculated with nonlinear regression using GraphPad Prism (version 6.0, San Diego, CA, USA).

Time- and Concentration-dependent MDR Reversal Assays. The ability to reverse ABCG2-mediated multidrug resistance of MDCK II BCRP cells toward the cytotoxic substrate SN-38 was investigated for the most potent compounds. The MTT cell viability assay was extended by addition of 20 µL of a 0 µM, 0.01 µM, 0.1 µM, 1 µM, and 10 µM dilution of the tested compounds in combination with 20 µL of a dilution series of SN-38 ranging from 0.1 µM to 100 µM (concentration-dependent assay). For the time-dependent assay we added 20 µL of the compound dilution series using concentrations of 0 µM, 0.1 µM, 0.25 µM, and 0.5 µM and 20 µl of a fixed concentration of 5 µM of SN-38 in a 96 well tissue culture plate (Starlab GmbH, Hamburg, Germany). A positive control was performed using MDCK parental cell line without the addition of the modulator. An amount of 160 µL of cell suspension was subsequently added to the wells resulting in a cell density of 2,000 cells per well for the concentration-dependent assay and 10,000 (day 1), 5,000 (day 2), 2,000 (day 3), 1,000 (day 4), 500 (day 5), 300 (day 6), 200 (day 7) for the time-dependent assay. In the concentration-dependent assay, the plates were incubated for 72 h at 37 °C and 5% CO_2 and were prepared and measured as described earlier for MTT assay. In the time-dependent assay, the cell viability was measured every day for a time period of 7 days.

Western Blotting of ABCG2. As much as 86,000 MDCK II BCRP cells were seeded out into T25 flasks for 4 day analysis, and 17,200 cells for 7 days, respectively. After adhering, cells were incubated with compound **19** (10 nM) and/or cytostatic drug **4** (0.5 µM). After 4 and 7 days, cells were lysed using Invitrogen Cell Extraction Buffer (Thermo Fisher Scientific Inc, Waltham, MA USA), supplemented with Halt Protease

Inhibition Cocktail (Thermo Fisher Scientific Inc, Waltham, MA USA) and PMSF (Thermo Fisher Scientific Inc, Waltham, MA USA), according to the manufacturer's instructions. Protein amount was measured by Pierce BCA Protein Assay Kit (Thermo Fisher Scientific Inc, Waltham, MA USA) and 15 µg protein of each sample were analyzed by SDS-PAGE using 10% stainfree precast gels (BioRad Lab GmbH, Munich, Germany) followed by total protein normalization. Transfer to a PVDF membrane (Thermo Fisher Scientific Inc, Waltham, MA USA) was conducted using 100 V and 350 mA for 1 h. After blocking, the membrane was incubated with primary anti-ABCG2 mouse antibody BXP-21 (Santa Cruz Biotechnology, Dallas, TX, USA) in a 1:200 dilution over night at 4 °C. The next day, secondary anti-mouse antibody m-IgGk BP-HRP (Santa Cruz Biotechnology, Dallas, TX, USA) was added in a 1:10000 dilution for 1.5 h. Luminescence visualization was performed using Clarity Western ECL Blotting Substrates (BioRad Lab GmbH, Munich, Germany), ChemiDoc XRS+ Imaging Acquiring System and Image Lab Software (BioRad Lab GmbH, Munich, Germany). The ABCG2 bands were related to total protein amount, measured by stain-free total protein normalization.

Confocal Laser Scanning Microscopy. Confocal laser scanning microscopy was used to get an optical evidence of accumulation of fluorescent compound **38** and thereby investigate its transport by ABCG2 as already described before.[58] For each probe 1 x 10^5 MCF-7 and MCF-7/MX were seeded into low µ-dish (ibidi GmbH, München, Germany) for 48 h. After reaching a confluence of 50-60%, the medium was changed to KHB. Afterwards, compound **38** or/and pheophorbide A were added up to a

concentration of 1 μM (compound **38**) and 0.5 μM (pheophorbide A) and a final volume of 900 μL. After the cells were incubated for 2 h at 37 °C and 5% CO_2, the fluorescence was measured at an excitation wavelength of 405 nm and emission filter of 500-530 nm (compound **38**) and 662-737 nm (pheophorbide A). For the measurement Nikon A1 R microscope (Nikon, Düsseldorf, Germany) tempered at 37 °C and its visualization software Nikon NIS Elements (Nikon, Düsseldorf, Germany) were used.

Molecular modelling studies

Human ABCG2 in complex with the fumitremorgin C-related inhibitor, MZ29 (PDB ID 6FFC) was crystallized using cryo-electron microscopy (cryo-EM).[100,101] The structure was downloaded from RCSB Protein Data Bank (PDB) and prepared and protonated using the protein structure preparation and Protonate3D modules implemented in Molecular Operating Environment (MOE) 2018.01, respectively.[103] The prepared transporter structure of the human ABCG2 was applied for flexible ligand docking using LeadIT from BioSolveIT, GmbH Germany.[104] During the docking simulations, the ligands were fully flexible while the residues of the receptor were treated as rigid. The binding site for the receptor was defined in 20 Å spacing of the amino acid residues centered based on the ligand, MZ29. The selected compound was docked using FlexX module implemented in LeadIT and predicted the binding mode in the binding site of the transporter.[105] For docking and scoring, the default parameters were applied, and top 100 highest scoring docked poses were stored for further analysis. Each receptor–

ligand complex having the lowest binding free energy of interactions was visualized using MOE2018.01 and selected the putative binding mode of the docked compound.[94]

Ancillary Information

Supporting Information

Molecular formula strings and the biological data (CSV)

LC-MS data of target compounds **18**-**40** (pdf)

Accession Codes

PDB accession code: 6FFC (**19**). Authors will release the atomic coordinates upon article publication.

Author Information

Corresponding authors

* E-mail: mwiese@uni-bonn.de

* E-Mail: s.m.stefan@medisin.uio.no

Current Author Address

Sven Marcel Stefan, Translational Neurodegeneration Research and Neuropathology Lab, Department of Neuro-/Pathology, University of Oslo, Oslo, Norway

Author Contributions

Katja Silbermann, Jiyang Li: These authors contributed equally.

Acknowledgement

The financial support provided by China Scholarship Council (CSC) is acknowledged.

Abbreviations Used

A2780/ADR, adriamycin-(doxorubicin)-selected A2780 cells; ABC, ATP-binding cassette; BCRP, breast cancer resistance protein; $c_{½tmax}$, concentration of reverser needed to reach ½ of tmax with antineoplastic agent in combination with sensitizer to half-maximally kill cancer cells (half-maximal cell death acceleration concentration); calcein AM, calcein acetoxymethyl ester; cryo-EM, cryogenic electron microscopy; c_{tmin}, concentration of reverser needed to reach minimum time needed for antineoplastic agent in combination with sensitizer to half-maximally kill cancer cells; EC_{50} = half-maximal effect concentration; GFP, green fluorescent protein; GI_{50}, half-maximal growth inhibition concentration; I_{max} = maximal inhibition level; MDCK, madin-darby canine kidney; MTT, (3-(4,5-dimethylthiazol-2-yl)-2,5-diphenyltetrazolium bromide); MCF-7/MX, mitoxantrone-selected Michigan Cancer Foundation-7 cells; MDR, multidrug resistance; MRP1, multidrug resistance-associated protein 1; P-gp, P-glycoprotein; TKI, tyrosine kinase inhibitor; t_{max}, time needed for antineoplastic agent alone at fixed concentration to half-maximally kill cancer cells; t_{min}, minimum time needed for antineoplastic agent in combination with sensitizer to half-maximally kill cancer cells; v_{max}, maximal transport velocity.

References

(1) Stavrovskaya, A. A.; Rybalkina, E. Y. Recent advances in the studies of molecular mechanisms regulating multidrug resistance in cancer cells. *Biochemistry (Mosc)* **2018**, *83*, 779–786.

(2) Triller, N.; Korosec, P.; Kern, I.; Kosnik M.; Debaljak, A. Multidrug resistance in small cell lung cancer: expression of P-glycoprotein, multidrug resistance protein 1 and lung resistance protein in chemo-naive patients and in relapsed disease. *Lung Cancer* **2006**, *54*, 235–240.

(3) Sedlakova, I.; Lavo, J.; Caltova, K.; Cervinka, M.; Tosner, J.; Rezac A.; Spacek, J. Clinical significance of the resistance proteins LRP, Pgp, MRP1, MRP3, and MRP5 in epithelial ovarian cancer. *Int. J. Gynecol. Cancer* **2015**, *25*, 236–243.

(4) Zeng, D.-F.; Zhang, J.; Zhu, L.-D.; Kong, P.-Y.; Li, J.-P.; Zhang, X.; Xu, W.; Wang, J.-L.; Pen, X.-G.; Wang P.; Liu, S.-H. Analysis of drug resistance-associated proteins expressions of patients with the recurrent of acute leukemia via protein microarray technology. *Eur. Rev. Med. Pharmacol. Sci.* **2014**, *18*, 537–543.

(5) Grogan, T. M.; Spier, C. M.; Salmon, S. E.; Matzner, M.; Rybski, J.; Weinstein, R. S.; Scheper, R. J.; Dalton, W. S. P-glycoprotein expression in human plasma cell myeloma: correlation with prior chemotherapy. *Blood* **1993**, *81*, 490–495.

(6) Steinbach, D.; Sell, W.; Voigt, A.; Hermann, J.; Zintl, F.; Sauerbrey, A. BCRP gene expression is associated with a poor response to remission induction therapy in childhood acute myeloid leukemia. *Leukemia* **2002**, *16*, 1443–1447.

(7) Damiani, D.; Tribelli, M.; Calistri, E.; Geromin, A.; Chiarvesio, A.; Michelutti, A.; Cavallin, M.; Fanin, R. The prognostic value of P-glycoprotein (ABCB) and breast cancer resistance protein (ABCG2) in adults with de novo acute myeloid leukemia with normal karyotype. *Haematologica* **2006**, *91*, 825−828.

(8) Lee, S. H.; Kim, H.; Hwang, J.-H.; Lee, H. S.; Cho, J. Y.; Yoon, Y.-S.; Han, H.-S. Breast cancer resistance protein expression is associated with early recurrence and decreased survival in resectable pancreatic cancer patients. *Pathol. Int.* **2012**, *62*, 167−175.

(9) Sun, S.; Cai, J.; Yang, Q.; Zhu, Y.; Zhao, S.; Wang, Z. Prognostic value and implication for chemotherapy treatment of ABCB1 in epithelial ovarian cancer: a meta-analysis, *PLoS One* **2016**, *11*, e0166058, 1−24.

(10) Gregorcyk, S.; Kang, Y.; Brandt, D.; Kolm, P.; Singer, G.; Perry, R. R. P-glycoprotein expression as a predictor of breast cancer recurrence. *Ann. Surg. Oncol.* **1996**, *3*, 8−14.

(11) Filipits, M.; Pohl, G.; Rudas, M.; Dietze, O.; Lax, S.; Grill, R.; Pirker, R.; Zielinski, C. C.; Hausmaninger, H.; Kubista, E.; Samonigg, H.; Jakesz, R. Clinical role of multidrug resistance protein 1 expression in chemotherapy resistance in early-stage breast cancer: the Austrian breast and colorectal cancer study group. *J. Clin. Oncol.* **2005**, *23*, 1161−1168.

(12) Matsuo, K.; Eno, M. L.; Ahn, E. H.; Shahzad, M. M.; Im, D. D.; Rosenein, N. B.; Sood, A. K. Multidrug resistance gene (MDR-1) and risk of brain metastasis in epithelial ovarian, fallopian tube, and peritoneal cancer. *Am. J. Clin. Oncol.* **2011**, *34*, 488−493.

(13) Robey, R. W.; Polgar, O.; Deeken, J.; To, K. W.; Bates, S. E. ABCG2: determining its relevance in clinical drug resistance. *Cancer Metastasis Rev.* **2007**, *26*, 39–57.

(14) Mao, Q.; Unadkat, J. D. Role of the breast cancer resistance protein

(BCRP/ABCG2) in drug transport – an update. *AAPS J.* **2015**, *17*, 65−82.

(15) Hardwick, L. J. A.; Velamakanni, S.; van Veen, H. W. The emerging pharmacotherapeutic significance of the breast cancer resistance protein (ABCG2). *Br. J. Pharmacol.* **2007**, *151*, 163–174.

(16) Möbus, V.; Pfaff, P. N.; Volm, T.; Kreienberg, R.; Kaubitzsch, S. Long time therapy with topotecan in patients with recurrence of ovarian carcinoma. *Anticancer Res.* **2001**, *21*, 3551–3556.

(17) O'Brien, M.; Eckardt, J.; Ramlau, R. Recent advances with topotecan in the treatment of lung cancer. *Oncologist* **2007**, *12*, 1194–1204.

(18) Galdy, S.; Cella, C. A.; Spada, F.; Murgioni, S.; Frezza, A. M.; Ravenda, S. P.; Zampino, M. G.; Fazio, N. Systematic therapy beyond first-line in advanced gastric cancer: an overview of the main randomized clinical trials. *Crit. Rev. Oncol. Hematol.* **2016**, *99*, 1–12.

(19) Kawabata, S.; Oka, M.; Shiozawa, K.; Tsukamoto, K.; Nakatomi, K.; Soda, H.; Fukuda, M.; Ikegami, Y.; Sugahara, K.; Yamada, Y.; Kamihira, S.; Doyle, L. A.; Ross, D. D.; Kohno, S. Breast cancer resistance protein directly confers SN-38 resistance of lung cancer cells. *Biochem. Biophys. Res. Commun.* **2001**, *280*, 1216–1223.

(20) Maliepaard, M.; van Gastelen, M. A.; de Jong, L. A.; Pluim, D.; van Waardenburg, R. A. M.; Ruevekamp-Helmers, M. C.; Floot, B. G. J.; Schellens, J. H. M. Overexpression of the *BCRP/MXR/ABCP* gene in a topotecan-selected ovarian tumor cell line. *Cancer Res.* **1999**, *59*, 4559–4563.

(21) Takagi, K; Dexheimer, . T. S.; Redon, C.; Sordet, O.; Agama, K.; Lavielle, G.; Pierre, A.; Bates, S. E.; Pommier, Y. Novel-E-ring camptothecin keto analogues (S38809 and S39625) are stable, potent, and selective topoisomerase I inhibitors without being substrates of drug efflux transporters. *Mol. Cancer Ther.* **2007**, *6*, 3229–3238.

(22) Yang, C.-H.; Schneider, E.; Kuo, M.-L.; Volk, E. L.; Rocchi, E.; Chen, Y.-C. BCRP/MXR/ABCP expression in topotecan-resistant human breast carcinoma cells. *Biochem. Pharmacol.* **2000**, *60*, 831–837

(23) Schellens, J. H. M.; Maliepaard, M.; Scheper, R. J.; Scheffer, G. L.; Jonker, J. W.; Smit, J. W.; Beijnen, J. H.; Schinkel, A. H. Transport of topoisomerase I inhibitors by the breast cancer resistance protein. *Ann. N. Y. Acad. Sci.* **2000**, *922*, 188–194.

(24) Ishii, M.; Iwahana, M.; Mitsui, I.; Minami, M.; Imagawa, S.; Tohgo, A.; Ejima, A. Growth inhibitory effect if a new campthotecin analog, DX-8951f, on various drug-resistant sublines including BCRP-mediated camptothecin derivative-resistant variants derived from the human lung cancer cell Line PC6. *Anticancer Drugs* **2000**, *11*, 353–362.

(25) Bessho, Y.; Oguri, T.; Achiwa, H.; Muramatsu, H.; Maeda, H.; Niimi, T.; Sato, S.; Ueda, R. Role of ABCG2 as biomarker for predicting resistance to CPT11/SN-38 in lung cancer. *Cancer Sci.* **2006**, *97*, 192–198.

(26) Nagashima, S.; Soda, H.; Oka, M.; Kitazaki, T.; Shiozawa, K.; Nakamura, Y.; Takemura, M.; Yabuuchi, H.; Fukuda, M.; Tsukamoto, K.; Kohno, S. BCRP/ABCG2

levels account for the resistance to topoisomerase I inhibitors and reversal effects by gefitinib in non-small cell lung cancer. *Cancer Chemother. Pharmacol.* **2006**, *58*, 594–600.

(27) Bates, S. E.; Medina-Perez, M.; Kohlhagen, G.; Antony, S.; Nadjem, T.; Robey, R. W.; Pommier, Y. ABCG2 mediates differential resistance to SN-38 (7-ethyl-10-hydroxycamptothecin and homocamptothecins. *J. Pharmacol. Exp. Ther.* **2004**, *310*, 836–842.

(28) Perego, P.; De Cesare, M.; De Isabella, P.; Carenini, N.; Beggiolin, G.; Pezzoni, G.; Plumbo, M.; Tartiglia, L.; Pratesi, G.; Pisano, C.; Carminati, P.; Scheffer, G. L.; Zunino, F. A novel 7-modified camptothecin analog overcomes breast cancer resistance protein-associated resistance in a mitoxantrone-selected colon carcinoma cell line. *Cancer Res.* **2011**, *61*, 6034–6037.

(29) Maliepaard, M.; van Gastelen, M. A., Tohgo, A.; Hausheer, F. H.; van Waardenburg, R. C. A. M.; de Jong, L. A.; Pluim, D.; Beijnen, J. H.; Schellens, J. H. M. Circumvention of breast cancer resistance protein (BCRP)-mediated resistance to camptothecins *in vitro* using non-substrate drugs or the BCRP inhibitor GF120918. *Clin. Cancer Res.* **2001**, *7*, 935–941.

(30) van Hattum, A. H.; Hoogsteen, J. J.; Schüper, H. M. M.; Maliepaard, M.; Scheffer, G. L.; Scheeper, R. J.; Kohlhagen, G.; Pommier, Y.; Pinedo, H. M.; Boven, E. Induction of breast cancer resistance protein by the camptothecin derivative DX-895 I f is associated with minor reduction of antitumor activity. *Br. J. Cancer* **2002**, *87*, 665–672.

(31) van Hattum, A. H.; Schülper, H. M. M.; Hausheer, F. H.; Pinedo, H. M.; Boven, E. Novel camptothecin derivative BNP1350 in experimental human ovarian cancer: determination of efficacy and possible mechanisms of resistance. *Int. J. Cancer* **2002**, *100*, 22–29.

(32) Erlichman, C.; Boerner, S. A.; Hallgren, C. G.; Spieker, R.; Wang, X.-Y.; James, C. D.; Scheffer, G. L.; Maliepaard, M.; Ross, D. D.; Bible, K. C.; Kaufmann, S. H. The HER tyrosine kinase inhibitor CI1033 enhances cytotoxicity of 6-ethyl-10-hydroxycamptrothecin and topotecan by inhibiting breast cancer resistance-mediated drug efflux. *Cancer Res.* **2001**, *61*, 739–748.

(33) Wang, X.-K.; To, K. K. W.; Huang, L.-Y.; Xu, J.-H.; Yang, K.; Wang, F.; Huang, Z.-C.; Ye, S.; Fu, L.-W. Afatinib circumvents multidrug resistance via dually inhibiting ATP binding cassette subfamily G member 2 in vitro and in vivo. *Oncotarget* **2014**, *5*, 11971−11985.

(34) Yang, K.; Chen, Y.; To, K. K. W.; Wang, F.; Li, D.; Chen, L.; Fu, L. Alectinib (CH5424802) antagonizes ABCB1- and ABCG2-mediated multidrug resistance *in vitro*, *in vivo* and *ex vivo*. *Exp. Mol. Med.* **2017**, *49*, e303, 1−13.

(35) Zhang, G.-N.; Zhang, Y.-K.; Wang, Y.-J., Barbuti, A. M., Zhu, X.-J., Yu, X.-Y.; Wen, A.-W., Wurpel, J. N. D.; Chen, Z.-S. Modulating the function of ATP-binding cassette subfamily G member 2 (ABCG2) inhibitor cabozantinib. *Pharmacol. Res.* **2017**, *119*, 89−98.

(36) Shi, Z.; Tiwari, A. K.; Shukla, S.; Robey, R. W.; Kim, I.-W.; Parmar, S.; Bates, S.

E.; Si, Q.-S.; Goldblatt, C. S.; Abraham, I.; Fu, L.-W., Ambudkar, S. V.; Chen, Z.-S. Inhibiting the function of ABCB1 and ABCG2 by the EGFR tyrosine kinase inhibitor AG1478. *Biochem. Pharmacol.* **2009**, *77*, 781−793.

(37) Ji, Y.; Yang, N.; Cai, C.-Y., Lei, Z.-Y.; Wang, J.-Q.; Gupta, P.; Teng, Q.-X.; Chen, Z.-S.; Kong, D.; Yang, D.-H. VS-4718 antagonizes multidrug resistance in ABCB1- and ABCG2-overexpressing cancer cells by inhibiting the efflux function of ABC transporters. *Front. Pharmacol.* **2018**, *9*, 1236, 1−12.

(38) Hu, J.; Zhang, X.; Wang, F.; Wang, X.; Yang, K.; Xu, M.; To, K. K. W.; Li, Q.; Fu, L. Effect of ceritinib (LDK378) on enhancement of chemotherapeutic agents in ABCB1 and ABCG2 overexpressing cells in vitro and in vivo. *Oncotarget* **2015**, *6*, 44643−44659.

(39) Donfrancesco, A.; De Ioris, M. A.; McDowell, H. P.; De Pasquale, M. D.; Ilari, I.; Jenker, A.; Castellano, A.; Cialfi, S., De Laurentis, C.; Dominici, C. Gefitinib in combination with oral topotecan and cyclophosphamide in relapsed neuroblastoma: pharmacological rationale and clinical response. *Pediatr. Blood. Cancer* **2010**, *54*, 55−61.

(40) Lhereux, S.; Krieger, S.; Weber, B.; Pautier, P.; Fabbro, M.; Selle, F.; Bourgeois, H.; Petit, T.; Lortholary, A.; Plantade, A.; Briand, M.; Leconte, A.; Richard, N.; Vilquin, O.; Clarisse, B.; Blanc-Fournier, C.; Joly, F. Expected benefits of topotecan combined with lapatinib in recurrent ovarian cancer according to biological profile: a phase 2 trial. *Int. J. Gynecol. Cancer.* **2012**, *22*, 1483–1488.

(41) Weroha, S. J.; Oberg, A. L.; Ziegler, K. L. A.; Dakhim, S. R.; Rowland, K. M.; Hartmann, L. C.; Moore Jr., D. F.; Keeney, G. L.; Peethambaram, P. P.; Haluska, P. Phase II trial of lapatinib and topotecan (LapTop) in patients with platinum-refractory/resistant ovarian and primary peritoneal carcinoma. *Gynecol. Oncol.* **2011**, *122*, 116–120.

(42) Wang, L.; Liang, L.; Yang, T.; Qiao, Y.; Xia, Y.; Liu, L.; Li, C.; Lu, P.; Jjiang, X. A pilot clinical study of apatinib plus irinotecan in patients with recurrent high-grade glioma. *Medicine (Baltimore)* **2017**, *96*, e9053, 1–5.

(43) Furman, W. L.; Navid, F.; Daw, N. C.; McCarville, M. B.; McGregor, L. M.; Spunt, S. L.; Rodriguez-Galindo, C.; Panetta, J. C.; Crews, K. R.; Wu, J.; Gajjar, A. J.; Houghton, P. J.; Santana, V. M.; Stewart, C. F. Tyrosine kinase inhibitor enhances the bioavailability of oral irinotecan in pediatric patients with refractory solid tumors. *J. Clin. Oncol.* **2009**, *27*, 4599−4604.

(44) Hoff, P. M.; Wolff, R. A.; Boogaard, K.; Waldrum, S.; Abbruzzese, J. L. A phase I study of escalating doses of the tyrosine kinase inhibitor semaxanib (SU5416) in combination with irinotecan in patients with advanced colorectal carcinoma. *Jpn. J. Clin. Oncol.* **2006**, *36*, 100−103.

(45) Boven, E.; Massard, C.; Armand, J. P.; Tillier, C.; Hartog, V.; Brega, N. M.; Countouriotis, A. M.; Ruiz-Garcia, A.; Soria, J. C. A phase I, dose-finding study of sunitinib in combination with irinotecan in patients with advanced solid tumors. *Br. J. Cancer* **2010**, *103*, 993−1000.

(46) Reardon, D. A.; Vredenburgh, J. J.; Coan, A.; Desjardins, A.; Peters, K. B., Guruangan, S.; Sathornsumetee, S.; Rich, J. N.; Herndon, J. E.; Fiedman, H. S. Phase I study of sunitinib and irinotecan for patients with recurrent malignant glioma. *J. Neurooncol.* **2011**, *105*, 621−627.

(47) Fan, Y. F.; Zhang, W.; Zeng, L.; Lei, Z. N.; Cai, C. Y.; Gupta, P.; Yang, D. H.; Cui, Q.; Quin, Z. D.; Chen, Z. S.; Trombetta, L. D. Dacomitinib antagonizes multidrug resistance (MDR) in cancer cells by inhibiting the efflux activity of ABCB1 and ABCG2 transporters. *Cancer Lett.* **2018**, *421*, 186–198.

(48) To, K.K.; Poon, D.C.; Wei, Y.; Wang, F.; Lin, G.; Fu, L. Pelitinib (EKB-569) targets the up-regulation of ABCB1 and ABCG2 induced by hyperthermia to eradicate lung cancer. *Br. J. Pharmacol.* **2015**, *172*, 4089–4106.

(49) Mathias, T. J.; Natarjan, K.; Shukla, S.; Doshi, K.A.; Singh, Z. N.; Ambudkar, S.V.; Baer, M. R. The FLT3 and PDGFR inhibitor crenolanib is a substrate of the multidrug resistance protein ABCB1 but does not inhibit transport function at pharmacologically relevant concentrations. *Invest. New Drugs* **2015**, *33*, 300–309.

(50) Zhang, W.; Fan, Y. F..; Cai, C. Y.; Wang, J. Q.; Teng, Q. X.; Lei, Z. N.; Zeng, L.; Gupta, P.; Chen, Z. S.; Olmutinib (BI1482694/HM61713), a novel epidermal growth factor receptor tyrosine kinase inhibitor, reverses ABCG2-mediated multidrug resistance in cancer cells. *Front*. *Pharmacol*. **2018**, *9*, 1097

(51) Wu, Z.X.; Teng, Q.X.; Cai, C.Y.; Wang, J.Q.; Lei, Z. N.; Yang, Y.; Fan, Y. F.; Zhang, J. Y.; Li, J.; Chen, Z. S.; Tepotinib reverses ABCB1-mediated multidrug resistance in

cancer cells. *Biochem. Pharmacol.* **2019**, *166*, 120–127.

(52) To, K.K.; Poon, D.C.; Wei, Y.; Wang, F.; Lin, G.; Fu, L.W.; Vatalanib sensitizes ABCB1 and ABCG2-overexpressing multidrug resistant colon cells to chemotherapy under hypoxia. *Biochem. Pharmacol.* **2015**, *97*, 27–37.

(53) Juvale, K.; Wiese, M. 4-Substituted-2-phenylquinazolines as inhibitors of BCRP. *Bioorg. Med. Chem. Lett.* **2012**, *22*, 6766−6769.

(54) Juvale, K.; Gallus, J.; Wiese, M. Investigation of quinazolines as inhibitors of breast cancer resistance protein. *Bioorg. Med. Chem.* **2013**, *21*, 7858−7873.

(55) Krapf, M. K.; Wiese, M. Synthesis and biological evaluation of 4-anilino-quinazolines and –quinolines as inhibitors of breast cancer resistance protein (ABCG2). *J. Med. Chem.* **2016**, *59*, 5449−5461.

(56) Krapf, M. K.; Gallus, J.; Wiese, M. Synthesis and biological investigation of 2,4-substituted quinazolines as highly potent inhibitors of breast cancer resistance protein. *Eur. J. Med. Chem.* **2017**, *139*, 587−611.

(57) Krapf, M. K.; Gallus, J.; Wiese, M. 4-Anilino-2-pyridylquinazolines and –pyrimidines as highly potent and nontoxic inhibitors of breast cancer resistance protein (ABCG2). *J. Med. Chem.* **2017**, *60*, 4474−4495.

(58) Kraege, S.; Stefan, K.; Juvale, K.; Ross, T.; Willmes, T.; Wiese, M. The combination of quinazoline and chalcone moieties leads to novel potent heterodimeric modulators of breast cancer resistance protein (BCRP/ABCG2). *Eur. J. Med. Chem.* **2016**, *117*, 212−229.

(59) Krapf, M. K.; Gallus, J.; Namasivayam, V.; Wiese, M. 2,4,6-Substituted quinazolines with extraordinary inhibitory potency toward ABCG2. *J. Med. Chem.* **2018**, *61*, 7952–7976.

(60) Krapf, M. K., Gallus, J.; Vahdati, S.; Wiese, M. New inhibitors of breast cancer resistance protein (ABCG2) containing a 2,4-disubstituted pyridopyrimidine scaffold. *J. Med. Chem.* **2018**, *61*, 3389–3408.

(61) Krapf, M. K.; Gallus, J.; Spindler, A.; Wiese, M. Synthesis and biological evaluation of quinazoline derivatives - a SAR study of novel inhibitors of ABCG2. *Eur. J. Med. Chem.* **2019**, *161*, 506−525.

(62) Pick, A.; Klinkhammer, W.; Wiese, M. Specific inhibitors of the breast cancer resistance protein (BCRP). *Chem. Med. Chem.* **2010**, *5*, 1498−1505.

(63) Schmitt, S. M.; Stefan, K.; Wiese, M. Pyrrolopyrimidine derivatives as novel inhibitors of multidrug resistance-associated Protein 1 (MRP1, ABCC1). *J. Med. Chem.* **2016**, *59*, 3018−3033.

(64) Juvale, K.; Stefan, K.; Wiese, M. Synthesis and biological evaluation of flavones and benzoflavones as inhibitors of BCRP/ABCG2. *Eur. J. Med. Chem.* **2013**, *67*, 115–126.

(65) Stefan, K.; Schmitt, S. M.; Wiese, M. 9-Deazapurines as broad-spectrum inhibitors of the ABC transport proteins P-glycoprotein, multidrug resistance-associated protein 1, and breast cancer resistance protein. *J. Med. Chem.* **2017**, *60*, 8758−8780.

(66) Silbermann, K.; Stefan, S. M.; Elshawadfy, R.; Namasivayam, V.; Wiese, M.

Identification of thienopyrimidine scaffold as inhibitor of the ABC transport protein ABCC1 (MRP1) and related transporters using a combined virtual screening approach. *J. Med. Chem.* **2019**, *62*, 4383–4400.

(67) Robey, R. W.; Pluchino, K. M. ; Hall, M. D.; Fojo, A. T.; Bates, S. E.; Gottesman, M. M. Revisiting the role of ABC transporters in multidrug-resistance cancer. *Nat. Rev. Cancer* **2018**, *18*, 452–464.

(68) Liu, B.; Li, L.-J.; Gong, X.; Zhang, W.; Zhang H.; Zhao, L. Co-expression of ATP binding cassette transporters is associated with poor prognosis in acute myleoid leukemia. *Oncol. Lett.* **2018**, *15*, 452–464.

(69) Schumacher, T.; Krohn, M.; Hofrichter, J.; Lange, C.; Stenzel, J.; Steffen, J.; Dunkelmann, T.; Paarmann, K.; Fröhlich, C.; Uecker, A.; Plath, A. S.; Sommer, A.; Brüning, T.; Heinze, H. J.; Pahnke, J. ABC Transporters B1, C1 and G2 differentially regulate neuroregeneration in mice. *PLoS One,* **2012**, *7*, e35613.

(70) Bernstein, H. G.; Hölzl, G.; Dobrowolny, H.; Hildebrand, J.; Trübner, K.; Krohn, M.; Bogerts, N.; Pahnke, J. Vascular and extravascular distribution of the ATP-binding cassette transporters ABCB1 and ABCC1 in aged human brain and pituitary. *Mech. Ageing Dev.* **2014**, *141–142*, 12–21.

(71) Samant, M. D.; Jackson, C. M.; Felix, C. L.; Jones, A. J.; Goodrich, D. W.; Foster, B. A.; Huss. W. J. Multi-drug resistance ABC transporters inhibition enhances murine ventral prostate ste,/progenitor cell differentiation. *Stem Cells Dev.* **2015**, *24*, 1236–1251.

(72) Ahmed-Belkacem, A.; Pozza, A.; Macalou, S.; Perez-Victoria, J. M.; Boumendjel, A.; Di Pietro, A. Inhibitors of cancer cell multidrug resistance mediated by breast cancer resistance protein (BCRP/ABCG2). *Anticancer Drugs* **2006**, *17*, 239–243.

(73) Stefan, S. M. Multi-target ABC transporter modulators: what next and where to go? *Fut. Med. Chem.* **2019**, *11*, 2353–2358.

(74) Ozvegy-Laczka, C.; Hegedus, T.; Varady, G.; Ujhelly, O.; Schuetz, J. D.; Varadi, A.; Keri, G.; Orfi, L.; Nemet, K.; Sarkadi, B. High-affinity interaction of tyrosine kinase inhibitors with the ABCG2 multidrug transporter. *Mol. Pharmacol.* **2004**, *65*, 1485–1495.

(75) Pawarode, A.; Shukla, S.; Minderman, H.; Fricke, S. M.; Pinder, E. M.; O'Loughlin, K. L.; Ambudkar, S.V.; Baer, M. R.; Differential effects of the immunosuppressive agents cyclosporine A, tacrolimus and sirolimus on drug transport by multidrug resistance proteins. *Cancer Chemother. Pharmacol.* **2007***, 60*, 179–188.

(76) Ivnitski-Steele, I.; Larson, R. S.; Lovato, D.M.; Khawaja, H. M.; Winter, S. S.; Oprea, T. I.; Sklar, L. A.; Edwards, B. S. High-throughput flow cytometry to detect selective inhibitors of ABCB1, ABCC1, and ABCG2 transporters. *Assay Drug Dev. Technol.* **2008**, *6*, 263–276.

(77) Colabufo, N. A.; Pagliarulo, V.; Berardi, F.; Contino, M.; Inglese, C.; Niso, M.; Ancona, P.; Albo, G.; Pagliarulo, A.; Perrone, R. Bicalutamide failure in prostate cancer treatment: involvement of multi drug resistance proteins. *Eur. J. Pharmacol.* **2008**, *601*, 38−42.

(78) Dai, C. L.; Tiwari, A. K.; Wu, C. P.; Su, X. D.; Wang, S. R.; Liu, D. G.; Ashby Jr.,

C. R.; Huang, Y.; Robey, R. W.; Liang, Y. J.; Chen, L. M.; Shi, C. J.; Ambudkar, S. V.; Chen, Z. S.; Fu, L. W. Lapatinib (Tykerb, GW572016) reverses multidrug resistance in cancer cells by inhibiting the activity of ATP-binding cassette subfamily B member 1 and G member 2. *Cancer Res.* **2008**, *68*, 7905–7914.

(79) Ma, S. L.; Hu, Y. P.; Wang, F.; Huang, Z. C.; Chen, Y. F.; Wang, X. K.; Fu, L. W. Lapatinib antagonizes multidrug resistance-associated protein 1-mediated multidrug resistance by inhibiting its transport function. *Mol. Med.* **2014**, *20*, 390–399.

(80) Colabufo, N. A.; Berardi, F.; Perrone, M. G.; Cantore, M.; Inglese, C.; Niso, M.; Perrone, R. Multi-drug-resistance-reverting agents: 2-arylazole and 2-arylthiazole derivatives as potent BCRP or MRP1 inhibitors. *Chem. Med. Chem.* **2009**, *4*, 188–195.

(81) Mi, Y. J.; Liang, Y. J.; Huang, H. B.; Zhao, H. Y.; Wu, C.P.; Wang, F.; Tao, L. Y.; Zhang, C. Z.; Dai, C. L.; Tiwari, A. K.; Ma, X. X.; To, K. K.; Ambudkar, S. V.; Chen, Z. S.; Fu, L. W. Apatinib (YN968D1) reverses multidrug resistance by inhibiting the efflux function of multiple ATP-binding cassette transporters. *Cancer Res.* **2010**, *70*, 7981–7991.

(82) Krauze, A.; Grinberga, S.; Krasnova, L.; Adlere, I.; Sokolova, E.; Domracheva, I.; Shestakova, I.; Andzans, Z.; Duburs, G. Thieno[3,2-b]pyridines–a new class of multidrug resistance (MDR) modulators. *Bioorg. Med. Chem.* **2014**, *22*, 5860–5870.

(83) Teodori, E.; Contino, M.; Riganti, C.; Bartolucci, G.; Braconi, L.; Manett,i D.; Romanelli, M. N.; Trezza, A.; Anthanasios, A.; Spiga, O.; Perrone, M. G.; Giampietro, R.; Gazzano, E.; Salerno, M.; Colabufo, N. A.; Dei, S. Design, synthesis and biological

evaluation of stereo- and regioisomers of amino aryl esters as multidrug resistance (MDR) reversers. *Eur. J. Med. Chem.* **2019**, *182*, 111655.

(84) Antoni, F.; Bause, M.; Scholler, M.; Bauer, S.; Stark, S. A.; Jackson, S. M.; Manolaridis, I.; Locher, K. P.; König, B.; Buschauer, A.; Bernhardt, G. Tariquidar-related triazoles as potent, selective and stable inhibitors of ABCG2 (BCRP). *Eur. J. Med. Chem.* **2020**, *191*, 112133.

(85) Dai, C.-L.; Liang, Y.-J.; Wang, Y.-S.; Tiwari, A. K.; Yan, Y.-Y.; Wang, F.; Chen, Z.-S.; Tong, X.-Z.; Fu, L.-W. Sensitization of ABCG2-overexpressing cells to conventional chemotherapeutic agent by sunitinib was associated with inhibiting the function of ABCG2. *Cancer Lett.* **2009**, *279*, 74−83.

(86) Yuan, J.; Wong, I. L.; Jiang, T.; Wang, S. W.; Liu, T.; Wen, B. J.; Chow, L. M.; Wan Sheng, B. Synthesis of methylated quercetin derivatives and their reversal activities on P-gp- and BCRP-mediated multidrug resistance tumour cells. *Eur. J. Med. Chem.* **2012**, *54*, 413–422.

(87) Cheung, L.; Flemming, C. L.; Watt, F.; Masada, N.; Yu, D. M. T.; Huynh, T.; Conseil, G.; Tivnan, A.; Polinsky, A.; Gudkov, A. V.; Munoz, M. A.; Vishvanath, A.; Cooper, D. M. F.; Henderson, M. J.; Cole, S. P. C.; Fletcher, J. I.; Haber, M.; Norris, M. D. High-throughput screening identifies ceefourin 1 and ceefourin 2 as highly selective inhibitors of multidrug resistance protein 4 (MRP4). *Biochem. Pharmacol.* **2014**, *91*, 97–108.

(88) Gupta, P.; Zhang, Y.-K.; Zhang, X.-Y.; Wang, Y.-J.; Lu, K. W.; Hall, T.; Peng, R.;

Yang, D.-H.; Xie, N.; Chen, Z.-S. Voruciclib, a potent CDK4/6 inhibitor, antagonizes ABCB1 and ABCG2-mediated multi-drug resistance in cancer cells. *Cell. Physiol. Biochem.* **2018**, *45*, 1515−1528.

(89) Zhu, X.; Wong, I. L. K.; Chan, K. F.; Cui, J.; Law, M. C.; Chong, T. C.; Hu, X.; Chow, L. M. C.; Chan, T. H. Triazole bridged flavonoid dimers as potent, nontoxic, and highly selective breast cancer resistance protein (BCRP/ABCG2) inhibitors. *J. Med. Chem.* **2019**, *62*, 8578–8608.

(90) Wang, E.-J.; Casciano, C. N.; Clement, R. P.; Johnson, W. W: In vitro flow cytometry method to quantitatively assess inhibitors of P-glycoprotein. *Drug Metab. Dispos.* **2000**, *28,* 522–528.

(91) Wang, E.-J.; Casciano, C. N.; Casciano, R: P.; Johnson, W. W. Cooperativity in the Inhibition of P-glycoprotein-mediated daunorubicin transport: evidence for half-of-the-sites reactivity. *Arch. Biochem. Biophys.* **2000**, *383*, 91–98.

(92) Kühnle, M.; Egger, M.; Müller, C.; Mahringer, A.; Bernhardt, G.; Fricker, G.; König, B.; Buschauer, A. Potent and selective inhibitors of breast cancer resistance protein (ABCG2) derived from the P-glycoprotein modulator tariquidar. *J. Med. Chem.* **2009**, *52*, 1190–1197.

(93) Köhler, S. C.; Wiese, M. HM30181 derivatives as novel potent and selective inhibitors of the breast cancer resistance protein (BCRP/ABCG2). *J. Med. Chem.* **2015**, *58*, 3910–3921.

(94) Kraege, S.; Köhler, S. C.; Wiese, M. Acryloylphenylcarboxamides: a new class of

breast cancer resistance protein (ABCG2) modulators. *Chem. Med. Chem.* **2016**, *11*, 2422–2436.

(95) Kraege, S.; Stefan, K.; Köhler, S. C.; Wiese, M. Optimization of acryloylphenylcarboxamides as inhibitors of ABCG2 and comparison with acryloylphenylcarboxylates. *Chem. Med. Chem.* **2016**, *11*, 2547–2559.

(96) Garnier-Suillerot, A.; Marbeuf-Gueye, C.; Salerno, M.; Loetchutinat, C.; Fokt, I.; Krawczyk, M.; Krowalczyk, T.; Priebe, W. Analysis of drug transport kinetics in multidrug-resistant cells. Implications for drug action. *Curr. Med. Chem.* **2001**, *8*, 51–64.

(97) Schmitt, S. M.; Stefan, K.; Wiese, M. Pyrrolopyrimidine derivatives and purine analogs as novel activators of multidrug resistance-associated protein 1 (MRP1, ABCC1). *Biochim. Biophys. Acta* **2017**, *1859*, 69−79.

(98) Kruijtzer, C. M. F.; Beijnen, J. H.; Rosing, H.; ten Bokkel Huinink, W. W.; Schot, M.; Jewell, R. C.; Paul, E. M.; Schellens, J. H. M. Increased oral bioavailability of topotecan in combination with the breast cancer resistance protein and P-glycoprotein inhibitor GF120918. *J. Clin. Oncol.* **2002**, *20*, 2943–2950.

(99) Taylor, N. M. I.; Manolaridis, I.; Jackson, S. M.; Kowal, J.; Stahlberg, H.; Locher, K. P. Structure of the human multidrug transporter ABCG2. *Nature* **2017**, *546*, 504–509.

(100) Jackson, S. M.; Manolaridis, I.; Kowal, J.; Zechner, M.; Taylor, N. M. I.; Bause, M.; Bauer, S.; Bartholomaeus, R.; Bernhardt, G.; Koenig, B.; Buschauer, A.; Stahlberg,

H.; Altmann, K.-H.; Locher, K. P. Structural basis of small-molecule inhibition of human multidrug transporter ABCG2. *Nat. Struct. Mol. Biol.* **2018**, *25*, 333– 340.

(101) Pavek, P.; Merino, G.; Wagenaar, E.; Bolscher, E.; Novotna, M.; Jonker, J. W.; Schinkel, A. H. Human breast cancer resistance protein: interactions with steroid drugs, hormones, the dietary carcinogen 2-amino-1-methyl-6-phenylimidazo(4,5-b)pyridine, and transport of cimetidine. *J. Pharmacol. Exp. Ther.* **2005**, *312*, 144–152.

(102) Köhler, S. C.; Silbermann, K.; Wiese, M. Phenyltetrazolyl-phenylamides: substituent impact on modulation capability and selectivity toward the efflux protein ABCG2 and investigation of interaction with the transporter. *Eur. J. Med. Chem.* **2016**, *124*, 881–895.

(103) Molecular Operating Environment (MOE), 2018.01; Chemical Computing Group ULC: 1010 Sherbooke St. West, Suite #910, Montreal, QC, Canada, H3A 2R7, **2018**.

(104) LeadIT, version 2.3.2; BioSolveIT GmbH: Sankt Augustin, Germany, **2017**.

(105) Rarey, M.; Kramer, B.; Lengauer, T.; Klebe, G. A fast flexible docking method using an incremental construction algorithm. *J. Mol. Biol.* **1996**, *261*, 470– 489.

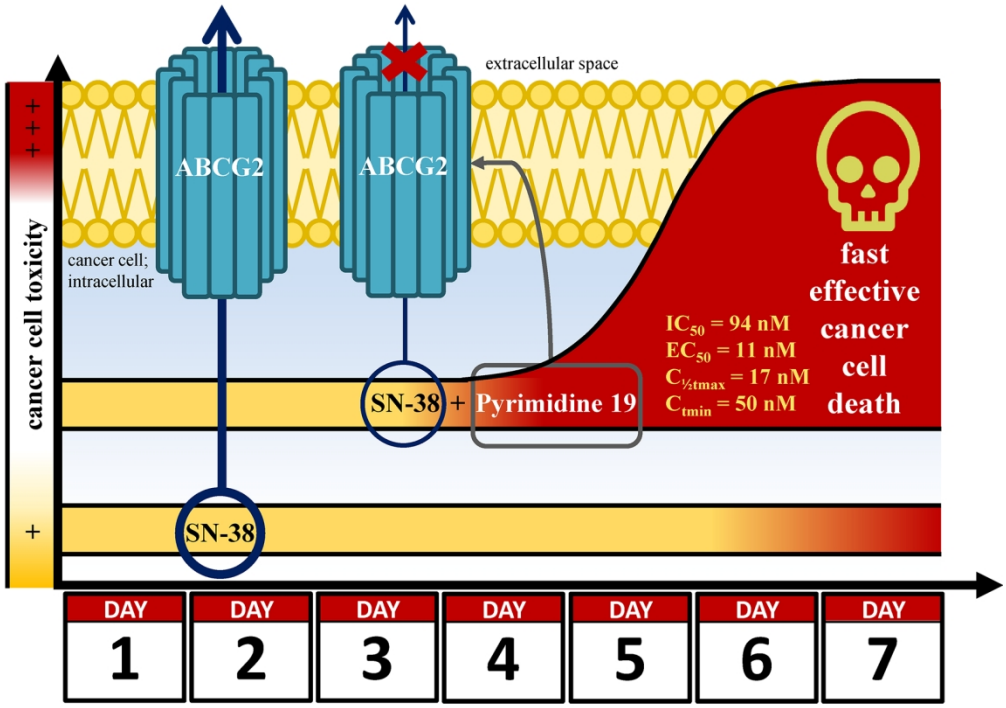
extracellular space
ABCG2
ABCG2
cancer cell; intracellular
cancer cell toxicity
+ + +
+
fast effective cancer cell death
IC50 = 94 nM
EC50 = 11 nM
C½tmax = 17 nM
Ctmin = 50 nM
SN-38 + Pyrimidine 19
SN-38
DAY 1
DAY 2
DAY 3
DAY 4
DAY 5
DAY 6
DAY 7

TOC Graphic